Document ID:EDF-4527
Revision ID:0
Effective Date:03/26/04

Engineering Design File

PROJECT NO. 23378

Revised Radiological Dose and Nonradiological Exposure Factors for In Situ Vitrification Loss of Confinement and Melt Expulsion Accident Scenarios at OU 7-13/14

INEEL
Idaho National Engineering and Environmental Laboratory

Form 412.14
10/9/2003
Rev. 05

ENGINEERING DESIGN FILE

EDF No.: 4527 EDF Rev. No.: 0 Project File No.: 23378

1. Title: Revised Radiological Dose and Nonradiological Exposure Factors for In Situ Vitrification Loss of Confinement and Melt Expulsion Accident Scenarios at OU 7-13/14

2. Index Codes:
Building/Type NA SSC ID NA Site Area

3. NPH Performance Category: _____ or ☐ N/A

4. EDF Safety Category: _____ or ☐ N/A SCC Safety Category: _____ or ☐ N/A

5. Summary:

In situ vitrification (ISV) has been proposed as a treatment option for portions of the Subsurface Disposal Area within the Radioactive Waste Management Complex at the Idaho National Engineering and Environmental Laboratory. The *Feasibility Study Preliminary Documented Safety Analysis for In Situ Vitrification at the Radioactive Waste Management Complex Subsurface Disposal Area* was performed earlier in which the gas-phase-release rates of contaminants were estimated for several postulated accident scenarios. This engineering design file documents revised radiological dose and nonradiological exposure factors for potential use in a future revision of the ISV Feasibility Study and Preliminary Documented Safety Analysis (FS-PDSA). Experimental and operational data are used to determine alternative values of material at risk, damage ratios, and airborne release factors for two accident scenarios: (1) unmitigated loss of confinement and (2) unmitigated melt expulsion.

Revised factors for these two scenarios are presented in Tables 1–3. In most instances, release fractions resulting from the revised factors are considerably lower than in the original FS-PDSA.

In the loss of confinement accident scenario, all species identified in the FS-PDSA (as being at risk of exceeding exposure limits) are estimated to be below the exposure limits if the revised exposure factors are used. In the melt expulsion accident scenario, several species identified by the FS-PDSA to be at risk of exceeding exposure limits (i.e., cadmium, carbon tetrachloride, potassium and sodium nitrates, hydrochloric acid, and phosgene) are estimated to be below the exposure limits if the revised exposure factors are used. However, test data suggest that more lead and cesium may be released than estimated in the original FS-PDSA.

It is recommended in future studies of nontraditional ISV that (1) better estimates of mass balances for organics and hydrochloric acid be obtained; (2) nontraditional ISV test data, when sufficiently plentiful, rather than data from traditional ISV tests be used to estimate destruction and retention efficiencies; (3) additional overburden be considered as a means to reduce the leak path factor; (4) the potential of radioactive contamination for collocated workers during a possible melt expulsion scenario be investigated further; (5) waste mapping be performed for potentially problematic types of waste; and (6) the potential escape of volatiles to surrounding ambient soil be mitigated through additional processing or be shown to not exist through testing. Extending the methodologies and principles used in this work to other accident scenarios is also briefly discussed.

6. Review (R) and Approval (A) and Acceptance (Ac) Signatures:
(See instructions for definitions of terms and significance of signatures.)

	R/A	Typed Name/Organization	Signature	Date
Performer/ Author	N/A	Todd T. Nichols/3F20	Todd T. Nichols	3/25/04
Performer/ Author	N/A	Charles M. Mohr/4662	Charles Mohr	3/25/04
Performer/ Author	N/A	Richard K. Farnsworth/3CH0	Richard Farnsworth	3/25/04
Technical Checker	R	Samuel C. Ashworth/3F20		3/25/04
Approver	A	David F. Nickelson/3F20		3/25/04

ENGINEERING DESIGN FILE

EDF No.: 4527 EDF Rev. No.: 0 Project File No.: 23378

1. Title: Revised Radiological Dose and Nonradiological Exposure Factors for In Situ Vitrification Loss of Confinement and Melt Expulsion Accident Scenarios at OU 7-13/14

2. Index Codes:
Building/Type NA SSC ID NA Site Area

Approver	A	Thomas E. Bechtold/3F20		03/25/04
Requestor	Ac	Brandt G. Meagher/3F20		3/26/04
Doc. Control		Bethl Lode		3/25/04

7. Distribution: (Name and Mail Stop)
T. T. Nichols, MS 3670; S. C. Ashworth, MS 3670; K. J. Holdren, MS 3920; C. M. Mohr, MS 3625; B. G. Meagher, MS 3920; T. E. Bechtold, MS 3920; R. K. Farnsworth, MS 2510; M. C. McQuiston, MS 3920; D. G. Abbott, MS 3425; D. F. Nickelson, MS 3670; T. J. Meyer, MS 3920

8. Does document contain sensitive unclassified information? ☐ Yes ☒ No
If Yes, what category:

9. Can document be externally distributed? ☒ Yes ☐ No

10. Uniform File Code: 6102 Disposition Authority: ENV1-h-1
Record Retention Period: See LST-9

11. For QA Records Classification Only: ☐ Lifetime ☒ Nonpermanent ☐ Permanent
Item and activity to which the QA Record apply:

12. NRC related? ☐ Yes ☒ No

13. Registered Professional Engineer's Stamp (if required)

N/A

CONTENTS

ACRONYMS 5

1. INTRODUCTION 7

2. OBJECTIVES 9

3. METHODOLOGY 10

3.1 Potential Waste Inventory Changes (Hydrofluoric Acid and Beryllium) 11

3.2 Escape of Volatiles to Surrounding Soil 11

4. QUALITY ASSURANCE 12

5. SCENARIO SPECIFIC DOSE AND EXPOSURE FACTORS 13

5.1 Unmitigated Loss of Confinement 13

5.1.1 MAR_i 13
5.1.2 DR_i = 1.7E-03 13
5.1.3 ARF_i 13
5.1.4 Impact on Dose and Exposure 14
5.1.5 Comparison with the Feasibility Study and Preliminary Documented Safety Analysis Approach 16

5.2 Unmitigated Melt Expulsion 16

5.2.1 MAR_i 16
5.2.2 DR_i = 8.2E-03 16
5.2.3 ARF_i 17
5.2.4 Comparison with the In Situ Vitrification Feasibility Study and Preliminary Documented Safety Analysis Approach 19

6. CONCLUSIONS 22

7. RECOMMENDATIONS 23

7.1 Improved Mass Balances 23

7.2 Nontraditional In Situ Vitrification 23

7.3 Better Estimate of LPF_i 24

7.3.1 Potential Revision of Leak Path Factor: Method 1—Extrapolate 10-cm Data 25
7.3.2 Potential Revision of Leak Path Factor: Method 2—Use Filtration Data Corresponding to Similar Depths 25

7.4 Radioactive Contamination 26

7.5 Waste Mapping 26

7.6 Escape of Volatiles to Surrounding Soil 27

7.7 Other Scenarios 27

8. REFERENCES 28

Appendix A—Equilibrium Modeling 31

Appendix B—Detailed Discussion of the Potential Escape of Volatile Organics to Surrounding Ambient Soil 59

Appendix C—Alternative Initiators for Hypothetical Idaho National Engineering and Environmental Laboratory Melt Expulsion 67

TABLES

1. Impact of proposed factor changes for loss of confinement scenario 15

2. Impact of proposed factor changes for melt expulsion scenario—Alternative 1 18

3. Impact of proposed factor changes for melt expulsion scenario—Alternative 2 20

ACRONYMS

ARF	airborne release factor
CF	conversion factor (1,000 mg/g)
DOE	U.S. Department of Energy
DR	damage ratio
EDF	engineering design file
FS-PDSA	feasibility study and preliminary documented safety analysis
INEEL	Idaho National Engineering and Environmental Laboratory
ISV	in situ vitrification
LLW	low-level waste
LPF	leak path factor
MAR	material at risk (Ci)
NTISV	nontraditional in situ vitrification
ORNL	Oak Ridge National Laboratory
OU	operable unit
RF	respirable fraction
RR	release rate (mg/second)
RT	release time (second)
RSAC	Radiological Safety Analysis Computer Program
RWMC	Radioactive Waste Management Complex
SDA	Subsurface Disposal Area
ST	source term (Ci)
TRU	transuranic

This page is intentionally left blank.

Revised Radiological Dose and Nonradiological Exposure Factors for In Situ Vitrification Loss of Confinement and Melt Expulsion Accident Scenarios at OU 7-13/14

1. INTRODUCTION

In situ vitrification (ISV) has been proposed as a treatment option for portions of the Operable Unit (OU) 7-13/14 Subsurface Disposal Area (SDA) within the Radioactive Waste Management Complex (RWMC) at the Idaho National Engineering and Environmental Laboratory (INEEL). The waste areas being considered for ISV processing include all of the transuranic (TRU) pits and trenches at the SDA as well as staged ISV processing of the waste packages currently stored on Pad A within the SDA.

In the ISV process, current between electrodes inserted into the ground causes ohmic heating, eventually forming a molten pool of glassy material that encapsulates and stabilizes contaminants in the waste. More detailed descriptions of the ISV process are found in *In Situ Vitrification of Transuranic Wastes: An Updated Systems Evaluation and Applications Assessment* (Buelt et al. 1987) and *Operable Unit 7-13/14 In Situ Vitrification Treatability Study Work Plan* (Farnsworth et al. 1999). The specific areas in the SDA under consideration for ISV treatment contain waste consisting primarily of contaminated combustibles, organic sludges, and nitrate salts.

Before ISV can be implemented, a safety analysis report must be prepared that addresses plausible accident scenarios and their consequences. An earlier feasibility study preliminary documented safety analysis (FS-PDSA) for ISV of the SDA is documented by Santee (2003). An important factor in contaminant release as estimated in the FS-PDSA, and in a future safety analysis report pertaining to the ISV process, is release of contaminants in the gas generated by the ISV process. All containerized waste disposed of in the treatment region of the SDA has the potential to generate gases. Thermal dissociation of sludge that contains nitrate salts can generate N_2, O_2, NO_x, and volatile nitrates and nitrites. Organic sludge and combustible waste can pyrolyze to form various gaseous products. Some types of organic waste contain volatile and semivolatile compounds that may be driven off before being modified by pyrolysis. In normal operation, a hood maintained at subatmospheric pressure covers the treatment area. Ambient air is introduced into the hood, diluting the off-gas and sweeping it into the gas treatment system.

The following accident scenarios have been postulated and their consequences estimated in the FS-PDSA:

1. *Loss of confinement.* Gaseous and suspended emissions from the ISV melt are normally contained by a hood and captured by an off-gas treatment system. Failure of the containment hood would result in a period of off-gas release to the atmosphere.

2. *Melt expulsion.* A violent upsurge of gas through the melt has the potential to elevate the hood and release both gaseous and entrained melt contaminants. This scenario has been observed during testing of ISV at the Oak Ridge National Laboratory (ORNL), as described in ORNL (1996).

3. *Drum deflagration.* Explosion of drum-confined oxygen or organic gases generated by nitrate dissociation and pyrolysis of organics or hydrogen produced by radiolysis of water or organics is postulated to damage electrodes and nearby waste containers. Drum deflagration is not postulated

to disrupt the melt or overburden, so delivery of additional contaminants to the surface does not seem likely.

4. *Underground fire.* Continual smoldering combustion of gases in the thermal front is listed as an accident scenario, but this could actually be considered normal operation when treating SDA regions containing both organic waste and nitrate salts. Volatile and semivolatile gases and pyrolysis products would be assumed to oxidize to their stoichiometric limit, and this assumption could be the basis for calculations used to estimate the equilibrium compositions of different mixtures of waste-generated gases at various temperatures.

5. *Direct radiation exposure.* This scenario results from exposure of workers when an unexpected strong radiation source is uncovered. This scenario does not involve the release of gases and entrained solids.

This engineering design file (EDF) applies specifically to Scenarios 1 and 2 (loss of confinement and melt expulsion), but the derived release factors pertaining to normal operations may also be applicable to the other accident scenarios involving the escape of off-gas (Scenarios 3 and 4). Results of this study are presented as alternative values for release factors presented in the FS-PDSA.

Several appendixes are included that provide greater details on subtopics in cases where only conclusions or results are presented in the body of this EDF. Appendix A explains the chemical equilibrium modeling performed, Appendix B discusses the potential for escape of volatiles to the surrounding ambient soil, and Appendix C provides an analysis of possible initiators of a melt expulsion at INEEL.

2. OBJECTIVES

The previous FS-PDSA did not base its estimate of gas composition and release rates on detailed analyses of the chemical and physical processes accompanying ISV. Rather, gross estimates of conversion fractions for reactions producing (or destroying) hazardous components and simplifying assumptions from sources not reflecting ISV experience were used. The purpose of this EDF is to provide revised factors that will be useful in evaluating radiological doses and nonradiological exposures that could result, without mitigation, from potential accident scenarios that have been pre-identified for ISV processing of buried waste at INEEL.

Detailed analysis of off-gas production and, where available, measurements from prior ISV testing are used to better bound the gas release characteristics of the two accident scenarios chosen for study—loss of confinement and melt expulsion. These two scenarios were chosen from the four involving gas release because the previous FS-PDSA showed they had the greatest potential for serious accident consequences. The results presented in this EDF may be used to support a future revision of the ISV FS-PDSA.

Although this EDF focuses on the loss of confinement and melt expulsion scenarios, some of the refined factors identified for these scenarios may also be applicable to the other pre-identified accident scenarios. Such potential applications are also briefly discussed in this EDF.

3. METHODOLOGY

A source term was determined, and the consequences of downwind radioactive material were calculated for each radioactive species in the FS-PDSA according to Equation (1):

$$ST = MAR \times DR \times ARF \times RF \times LPF \quad (1)$$

where

ST = source term (Ci)

MAR = material at risk (Ci)

DR = damage ratio

ARF = airborne release fraction

RF = respirable fraction

LPF = leak path factor.

Consequences of the estimated source term releases to the atmosphere were determined using the Radiological Safety Analysis Computer Program (RSAC) -6.

The release rate of each nonradioactive hazardous material was determined using Equation (2):

$$RR = (MAR)(CF)(DR)(ARF)(RF)(LPF)/(RT) \quad (2)$$

where

MAR, DR, ARF, RF, and LPF have the same meanings as in the source term equation, and

RR = release rate of each chemical (mg/second)

CF = conversion factor (1,000 mg/g)

RT = release time (second).

The downwind concentration (mg/m^3) of each hazardous species at different distances from the treatment area was calculated by multiplying the estimated release rates by a distance-specific atmospheric dispersion factor (s/m^3). The source term and release rate formalism plus the accident scenarios are described in more detail in the FS-PDSA and EDF-3563, "Radiological Dose and Nonradiological Exposure Calculations for ISV Accident Scenarios." Determination of the waste inventories is described in EDF-3543, "SDA Inventory Evaluation for ISG, ISV, and ISTD PDSA Source Terms."

This EDF uses experimental and operational data to determine alternative values of MAR, damage ratio, and ARF for some of the waste components for the loss of confinement and melt expulsion accident scenarios. Because of the multiplicative form of the source term and release rate equations, these changes in factor values result in equivalent changes to the corresponding source terms and release rates. Thus, the impact of the proposed factor changes are presented in terms of a ratio of the new (or revised)

over the old (or original from the FS-PDSA), ST_{new}/ST_{old} and RR_{new}/RR_{old} for the source term and release rate, respectively.

3.1 Potential Waste Inventory Changes (Hydrofluoric Acid and Beryllium)

In the FS-PDSA, hydrofluoric acid was determined to be at risk of exceeding exposure limits in both accident scenarios, and beryllium was determined to be at risk of exceeding exposure limits in the melt expulsion scenario. However, not all of the inventory for these two contaminants assumed by the FS-PDSA is slated for treatment by ISV. Some beryllium is planned to be grouted (HAD-268). It also appears that the only disposal locations within the SDA that have substantial quantities of beryllium are soil vault rows and certain trench locations (Holdren et al. 2002). The existing waste inventory shows that all the hydrofluoric acid disposed of within the SDA is buried in only four low-level waste (LLW) trenches (i.e., Trench 20, 27, 29, and 31), and ISV is not being considered as a treatment alternative for LLW trenches. Consequently, hydrofluoric acid and beryllium may be present in the waste inventory being considered for treatment by ISV in lesser amounts than assumed in the FS-PDSA. For comparison with the FS-PDSA, however, the impact of the revised exposure factors proposed here for these two contaminants is given assuming the same inventory levels (MAR_i) as used by the FS-PDSA.

3.2 Escape of Volatiles to Surrounding Soil

The *Preliminary Evaluation of Remedial Alternatives for the Subsurface Disposal Area* (Zitnik et al. 2002) recommends that in situ thermal desorption be used as a pretreatment for ISV, but the reasons are not clearly stated. The risk of volatiles outpacing the melt front and escaping to the surrounding soil, if credible, would need to be mitigated. This risk is addressed in detail in Appendix B. The potential escape of volatiles to the surrounding ambient soil, however, is not quantified in this EDF because of a lack of supporting site-specific data. Nor was such potential escape accounted for in the FS-PDSA.

4. QUALITY ASSURANCE

Except for the equilibrium calculations performed in Appendix A, all calculations in this EDF were performed on a hand calculator or in Microsoft EXCEL spreadsheets. This work is not being used to ensure that design or operational requirements are being met; therefore, MCP-2374, "Analyses and Calculations," does not apply.

The software HSC 5.11, *Outokumpu HSC Chemistry for Windows* (Outokumpu 2003), was the Gibbs minimization software used to estimate equilibrium of the various systems studied in Appendix A. However, because this work is a scoping study and its results are not being used to ensure that design or operational requirements are being met, MCP-3039, "Analysis Software Control," does not apply. Nonetheless, ASPEN Plus 11.1 (Aspen 2001) was used to validate HSC by running the simulation for the organic/acid system in both simulators in the temperature range 100–1,000°C. The organic/acid system was chosen for validation because of the large number of components involved (i.e., 45) and the sensitivity of the results to the thermodynamic data used. This offered the benefit of comparing results from two different databanks and solution algorithms. Because the species of concern are volatile, only the gas phase was considered in HSC. However, liquid-gas-phase partitioning for each component does not have to be prespecified in ASPEN Plus. The results from the two software programs were essentially identical. Both HSC and ASPEN Plus were used as procured from vendors and were not modified or customized. Therefore, the software is exempt from MCP-550, "Software Management."

5. SCENARIO SPECIFIC DOSE AND EXPOSURE FACTORS

5.1 Unmitigated Loss of Confinement

5.1.1 MAR_i

Buelt et al. (1987, pp. xii and 49–50) experimentally determined a minimum destruction efficiency of 96.6% for nitrates with a large-scale test of traditional ISV. Nitrates were effectively reduced to diatomic N_2 and O_2. These results are consistent with Gibbs minimization calculations performed in HSC that predict that the equilibrium quantity of HNO_3 in the waste is essentially zero for the temperature range 100–1,600°C. The experimental value of 96.6% is also consistent with Gibbs minimization calculations performed in HSC for sodium nitrate decomposition. However, the experimental value of 96.6% is higher than the 46% calculated by Gibbs minimization for potassium nitrate (see Appendix A). Consequently, 3.4% of the nitrates is assumed to be at risk of release and included in the MAR_i for $NaNO_3$ and HNO_3, and 46% is assumed for KNO_3.

5.1.2 DR_i = 1.7E-03

The steady-state amount of material being released into the hood is a smoothed value of the entire amount being released over the entire process duration; as such, the fraction of material involved in the accidental release (DR_i) is equal to the accident scenario's release duration divided by the time required to process the entire treatment area, and it is has the same value for all species. If we use the same assumptions as the FS-PDSA (p. 3-72) used (i.e., the ISV treatment area is 900 ft^2 and 10 ft thick, and the liquid melt has a density of 177 lb/ft^3), we assume a treatment mass of 722.6 metric tons (900 ft^2 × 10 ft × 177 lb/ft^3 / 2,204.6 lb/metric ton). In situ vitrification proceeds at a rate of 4-5 metric tons/hour (Dragun 1991), resulting in an estimated processing time of 160.6 hours (722.6 metric tons / 4.5 metric tons/hour) to melt the entire volume, which is consistent with the time window of 150–200 hours given by Dragun (1991). We assume a relatively short processing time of 150 hours to give a conservative (i.e., high) value of the damage ratio. Using the same release duration as the FS-PDSA for the loss of confinement scenario (i.e., 15 minutes) results in a DR_i value of 0.0017 ([15 minutes / 60 minutes/hour] / 150 hours).

5.1.3 ARF_i

5.1.3.1 Nonvolatiles (ARF_i = 1.8E-03). Operating factors that impact element retention in the melt include burial depth, gas generation rates, and depth of overburden (Buelt et al. 1987, p. xii; Geosafe 2001, p. 53). An overburden is not used with traditional top-down ISV; consequently, the average retention rate of nonvolatiles measured in traditional ISV tests can be used to conservatively estimate the ARF_i for a nonvolatile in nontraditional ISV (NTISV). Geosafe (2001) identified retention efficiencies for several species from several traditional ISV tests where most retention efficiencies were above 99.9%. However, to be conservative, the lowest retention listed is used as the universal retention efficiency for all nonvolatiles. The lowest retention mentioned by Geosafe (2001, pp. 52–53) is 99.82% for ruthenium in a 1983 pilot-scale test at Hanford. Consequently, the value of the universal ARF_i is 0.0018 (i.e., 1 - 0.9982).

5.1.3.2 Semivolatiles. Arsenic and cadmium have retention efficiencies greater than 80% with NTISV (Geosafe 1998, p. 6), which is consistent with the field test results of traditional ISV at Pacific Northwest Laboratory (i.e., 75–80% retention for cadmium) (Buelt et al. 1987, p. 53). Consequently, the lower, traditional ISV value of 75% will be assumed for arsenic and cadmium, resulting in a value of 0.25 (i.e., 1 - 0.75) for their ARF_i.

All of the mercury is expected to be volatilized (Geosafe 1998, p. 6; Farnsworth et al. 1999, p. C-22), so its ARF_i value is assumed to be 1, as was done in the FS-PDSA.

More than 90% of lead is retained in the melt during NTISV (Geosafe 1998, p. 6), which is consistent with the field test results of traditional ISV at Pacific Northwest Laboratory (i.e., 87.5–96.3% retention for lead) (Buelt et al. 1987, p. 53). Consequently, the lower, traditional ISV retention value of 87.5% will be assumed for lead, resulting in a value of 0.125 (1 - 0.875) for its ARF_i.

The retention of cesium is usually above 99.9% unless chlorides are present. Geosafe (2001, p. 53) reports results of a pilot-scale test performed at ORNL in 1991. Trace amounts of radioactive cesium were used with waste involving polyvinyl chloride pipe. The cesium retention efficiency was only 97.6%. It was concluded that the cesium metal reacted with the chlorides from the polyvinyl chloride, increasing the release of cesium because the volatility of the cesium-chloride compound is greater than the cesium element alone. Because chlorides are present in the waste, the larger, chloride-based ARF_i value of 0.024 (i.e., 1 - 0.976) is assumed.

The FS-PDSA assumed an ARF value of 1.0 for antimony. However, there is sufficient justification to revise this value. The boiling point for antimony is 1,380°C, which is far greater than that for cesium (boiling point = 670°C) and less than that for lead (boiling point = 1,620°C). Therefore, the amount of antimony volatilized during ISV processing should be between that of cesium (2.6%) and lead (12.5%). To be conservative, the higher ARF value of 0.125 was assumed for antimony.

The ratio of the ARF_i value of a semivolatile over that of the universal value for a solid quantitatively describes the increased entrainment of the semivolatile. Values of these normal operation entrainment ratios are given in Table 1.

5.1.3.3 Volatiles. Buelt et al. (1987, pp. xii and 49) experimentally determined a retention efficiency of 98.8% for fluorides with traditional ISV, but a description of the form of the fluorides included in the waste was not given. Gibbs minimization calculations performed in HSC predict that hydrofluoric acid is produced rather than consumed in the temperature range from 100–1,600° C (see Appendix A). Consequently, the ARF_i value is assumed to be 1.0 for hydrofluoric acid because of the uncertain applicability of the test data.

The value of the airborne release faction for all other volatiles is 1.0, as assumed in the FS-PDSA.

5.1.4 Impact on Dose and Exposure

The impact of the proposed factor changes is shown in Table 1. The new release rates relative to the old would result in exposure concentrations under the limits for those species that previously exceeded their limits (i.e., hydrofluoric acid, cadmium, phosgene, mercury, and formaldehyde) (Santee 2003, Table 3-27). However, two species (i.e., lead and cesium) would have exposure concentrations or dose equivalents considerably higher than previously determined. Despite this increase, lead will still be under the exposure limit for the extremely unlikely frequency category: the new estimated exposure, 16.8 mg/m^3 (i.e., 7.3 [from Table 1] multiplied by 2.3 [from Table 3-27 of the FS-PDSA]), is still below the collocated worker limit of 100.

Table 1. Impact of proposed factor changes for loss of confinement scenario.

Species	MAR_i[a]	DR_i[a]	ARF_i[a]	Entrainment Ratio	Exposure Ratio
Radionuclides					ST_{new}/ST_{old}
Cesium	No change	0.0017 (0.058)	0.024 (5.0E-04)	0.024/1.8E-03 = 13.3	1.4
All others			1.8E-03 (5.0E-04)	1.0	0.11
Hazardous species					RR_{new}/RR_{old}
Nonvolatiles					
Sodium nitrate	3.4% (100%)	0.0017 (0.058)	1.8E-03 (5.0E-04)	1.0	3.6E-03
Potassium nitrate	46% (100%)				4.9E-02
All others	No change				0.11
Semivolatiles					
Lead	No change	0.0017 (0.058)	0.125 (5.0E-04)	69.4	7.3
Arsenic			0.25 (1.0)	138.9	7.3E-03
Cadmium					
Antimony			0.125 (1.0)	69.4	3.6E-03
Mercury			No change (1.0)	555.6	0.029
Volatiles					
HNO_3	3.4% (100%)	0.0017 (0.058)	No change (1.0)	N/A	1.0E-03
Hydrofluoric acid	No change				0.029
Organics					
Pyrolysis Products					
HCl	N/A				0.029
Phosgene					

a. Original value from Santee (2003) is given in parenthesis.

ARF = airborne release factor
DR = damage ratio
MAR = material at risk
RR = release rate
ST = source term

Even if all the radionuclides had source terms 1.4 times greater than their previously determined values as predicted here for cesium, the predicted dose should still be under the 100-rem limit (1.4×38 [Table 3-26 from the FS-PDSA] = 53.2 < 100). The impact of the increased source term of cesium (and the decreased source term of all other radionuclides) on the estimated dose equivalent needs to be calculated in the RSAC computer program, however, to quantify and confirm the expected decrease in the predicted radiation dose.

5.1.5 Comparison with the Feasibility Study and Preliminary Documented Safety Analysis Approach

The differences with the FS-PDSA approach (Santee 2003) are (1) experimental destruction and retention efficiencies are used to revise the MAR_i and ARF_i factors for some species and (2) the damage ratio is an operational time ratio rather than an area ratio based on a hypothetical release pathway.

5.2 Unmitigated Melt Expulsion

Because the expelled glass remains relatively close to the treatment area (most of it simply overflows onto the surface ground), the contaminant releases to the atmosphere occur through the escaped gas. Gas escapes to the outside environment while the off-gas hood is raised off of the ground for a few seconds due to the resulting pressure surge.

A melt expulsion that occurred at the ORNL (1996) is assumed to be typical, as was assumed in the FS-PDSA. Additional overburden was not placed on top of the vitrification area prior to initiating ISV processing at ORNL, and additional overburden is not included in our analysis of this accident scenario.

5.2.1 MAR_i

The MAR_i for all species is the same as for normal operations (i.e., as in the loss of confinement scenario).[a] This differs from the FS-PDSA, which assumed only 50% destruction of organics and did not account for any destruction of nitrates.

5.2.2 DR_i = 8.2E-03

In the ORNL (1966, p. 26) event, 9,396 moles of gas were estimated to have escaped during the few seconds when the hood was lifted. Using the ideal gas law (PV = nRT), 272,287 standard cubic feet (scf) of gas escaped to the atmosphere. Energy calculations show that a maximum of 25 scf of gas is required to produce the melt expulsion (see Appendix C). Consequently, the majority of the gas (1 - 25/272,287 = 0.9999) that escapes to the atmosphere during a melt expulsion is gas from normal processing already resident in the hood when the accident occurs. The hood flow capacity at ORNL was 3,670 scf/minute; therefore, the amount of gas that escaped was 74.2 minutes worth of normal processing (i.e., 272,287 scf/3,670 scf/minute). The amount of gas that escapes during a melt expulsion corresponds to about 0.0082 (74.2 minute × [1 hour/60 minute]/150 hour) of the total gas produced during the 150 hours of the complete ISV treatment process. And because the escaped gas came from normal steady state processing, the escaped gas would be produced from treating 0.0082 of the treatment area. Consequently, the universal DR_i for all species is 8.2E-03.

a. Because the escaped gas is assumed to be from normal operations, organics are assumed to have the same destruction efficiency as in normal operations (i.e., 99%) (Santee 2003, p. 3-83).

5.2.3 ARF_i

5.2.3.1 Volatiles. The ARF_i for volatile species is the same as for normal operations (i.e., as in the loss of confinement scenario [$ARF_i = 1.0$]). This is the same as in the FS-PDSA.

5.2.3.2 Nonvolatiles and Semivolatiles. Assuming the melt expulsion of ORNL to be typical, the ratio of the mass of glass melt expelled (20 tons) over the total amount of melt processed is estimated to be 0.025 (Santee 2003, p. 3-72). However, most of the expelled glass flows onto the ground. Some glass (relatively little) splashes onto the hood equipment or is carried outside the hood during its brief lift, in the form of globs or hair-like fibers, by the escaping gas. The bulk flow of glass on the ground (i.e., the majority of the 20 tons expelled) does not contribute to contaminant release because it stays relatively close to the treatment area. Also, there is no mechanism for the constituents of bulk flow to partition to the gas phase.[b]

Possible entrainment from the expelled melt could occur during the few seconds when accelerated gas escapes between the hood foot and the melt-covered ground surface. If the physics of the escaping mechanism for the gas facilitated formation of aerosols, one would expect bound semivolatile cesium to partition from the entrained hair-like fibers into the carrier gas, resulting in the specific activity of cesium in the hair-like fibers to be less than that in the bulk flow. However, this did not happen at the ORNL incident. The ORNL (1996, p. 21) investigation determined that the specific activity of cesium (assumed to mean the activity of cesium per mass of total material) was the same in the bulk flow glass outside the hood, in the splattered glass on roughing filters inside the hood, and in the hair-like fiber glass found outside the hood. This suggests that, although the accelerated gas entrained melt chunks as it escaped through the narrow gap between the hood foot and ground surface, the entrained chunks cooled quickly and were not atomized or reduced to aerosols in the escaping gas.

Consequently, it appears that the melt expelled is not a source of significant contaminant release, and that the predominant source of contaminant release (i.e., volatile, semivolatile, and nonvolatile) is the escaped gas generated from normal processing and resident in the hood immediately before expulsion. Consequently, the ARF_i values for nonvolatile and semivolatile species could reasonably be assumed to be the same as those determined for the loss of confinement scenario (i.e., normal operating conditions).

5.2.3.2.1 Alternative 1—The ARF_i values for nonvolatile and semivolatile species are assumed to be the same as those determined for the loss of confinement scenario. This means that the rapid gas release does not result in any enhanced particulate entrainment (on a volumetric basis).

5.2.3.2.1.1 Impact on Dose and Exposure—The impact of proposed factor changes is shown in Table 2. The new source terms for all radionuclides, except cesium, are smaller than the old source terms (according to Table 3-22 of Santee [2003]). However, the new estimated dose will have to be computed in the RSAC computer program to confirm that the predicted dose will be below the exposure limit.

Lead was at the limit value for the extremely unlikely and unlikely frequency categories in Table 3-23 of the original FS-PDSA, and the factors proposed here result in an even greater release rate for lead. The new release rates relative to the old ones for hydrofluoric acid and uranium, although lower, would still result in collocated worker exposures higher than the exposure limits.

---

b. At melt temperatures of approximately 1,600°C, all unbound volatiles and semivolatiles would have volatilized before the expulsion.

Table 2. Impact of proposed factor changes for melt expulsion scenario—Alternative 1.

Species	MAR_i[a]	DR_i[a]	ARF_i[a]	Exposure Ratio
Radionuclides				ST_{new}/ST_{old}
Cesium	No change	0.0082 (0.025)	0.024 (5.0E-03)	1.57
All Others			1.8E-03 (5.0E-03)	0.12
Hazardous				RR_{new}/RR_{old}
Nonvolatiles				
Sodium nitrate	3.4% (100%)	0.0082 (0.025)	1.8E-03 (5.0E-03)	4.0E-03
Potassium nitrate	46% (100%)			5.4E-02
All others	No change			0.12
Semivolatiles				
Lead	No change	0.0082 (0.025)	0.125 (5.0E-03)	8.2
Arsenic			0.25 (1.0)	0.082
Cadmium				
Antimony			0.125 (1.0)	0.041
Mercury			No change (1.0)	0.328
Volatiles				
HNO3	3.4% (100%)	0.0082 (0.025)	No change (1.0)	0.011
Hydrofluoric acid	No change			0.328
Organics	1.0% (50%)			6.56E-03
Pyrolysis Products				
HCl	N/A			6.56E-03
Phosgene				

a. Original value from Santee (2003) is given in parenthesis.

ARF = airborne release factor
DR = damage ratio
MAR = material at risk
RR = release rate
ST = source term

The new release rates relative to the old ones for the other contaminants that exceeded their limits in the FS-PDSA (i.e., beryllium, cadmium, carbon tetrachloride, potassium nitrate, hydrochloric acid, sodium nitrate, and phosgene) result in predicted exposures lower than the exposure limits.

5.2.3.2.2 Alternative 2—Instead of assuming the ARF_i values for nonvolatile and semivolatile species to be the same as those determined for the loss of confinement scenario, one could be more conservative and, for a generic nonvolatile, follow the approach of the FS-PDSA. That approach used the $ARF_i = 0.005$ value from the DOE handbook, "Airborne Release Fractions/Rates and Respirable Fractions for Nonreactor Nuclear Facilities" (DOE-HDBK-3010-94), for ". . .accelerated gas flows in area without significant pressurization. . ." for nonvolatiles. Therefore, Alternative 2 does assume that particulate entrainment is enhanced somewhat by the rapid gas release.

To estimate the airborne release factor for the semivolatile species (i.e., cesium, lead, arsenic, cadmium, and antimony) that experimental testing has shown to have entrainment characteristics different than the typical solid, the generic value (0.005 from DOE-HDBK-3010-94) is multiplied by the normal operation entrainment ratio (given in the description of the loss of confinement scenario [see Table 1]).

However, all the entrained mercury is assumed to be airborne just as in normal operations; therefore, its $ARF_i = 1.0$, as in the loss of confinement scenario and as assumed in the FS-PDSA.

5.2.3.2.2.1 Impact on Dose and Exposure—The impact of the proposed factor changes is shown in Table 3. The new source terms for all radionuclides except cesium are smaller than the old, but not enough to get the collocated worker total effective dose under the limit (Santee 2003, Table 3-22). However, the new estimated dose will have to be computed in the RSAC computer program to quantify the predicted change in the dose exposure.

Lead was at the limit value for the extremely unlikely and unlikely frequency categories in Table 3-23 of the FS-PDSA, and the factors proposed here result in an even greater release rate for lead. Although lower, the new release rates relative to the old ones for beryllium, hydrofluoric acid, and uranium still result in collocated worker exposures higher than the exposure limits. The new release rates relative to the old ones for the other contaminants that exceeded their limits in the FS-PDSA (i.e., cadmium, carbon tetrachloride, potassium nitrate, hydrochloric acid, sodium nitrate, and phosgene) result in predicted exposures lower than the exposure limits.

Relative to Alternative 1, the more conservative Alternative 2 adds two entries to the list of exceeded limits (i.e., beryllium and the radioactive dose exposure).

5.2.4 Comparison with the In Situ Vitrification Feasibility Study and Preliminary Documented Safety Analysis Approach

The main difference between factors proposed in this EDF and those of the FS-PDSA are derived from differences in assumptions about the source of potential contaminant release. The FS-PDSA appears to assume the following:

- Escaped gas came from the event-inducing bubble and the 20 tons of expelled melt
- Entrained particles in the escaped gas came from the expelled melt.

Table 3. Impact of proposed factor changes for melt expulsion scenario—Alternative 2.

Species	MAR_i[a]	DR_i[a]	ARF_i[a]	Exposure Ratio
Radionuclides				ST_{new}/ST_{old}
Cesium	No change	0.0082 (0.025)	5.0E-03 × 13.3 = 6.65E-02 (5.0E-03)	4.36
All others			No change (5.0E-03)	0.33
Hazardous				RR_{new}/RR_{old}
Nonvolatiles				
Sodium nitrate	3.4% (100%)	0.0082 (0.025)	No change (5.0E-03)	0.011
Potassium nitrate	46% (100%)			0.15
All others	No change			0.33
Semivolatiles				
Lead	No change	0.0082 (0.025)	5.0E-03 × 69.4 = 0.347 (5.0E-03)	22.76
Arsenic			5.0E-03 × 138.9 = 0.695 (1.0)	0.23
Cadmium				
Antimony			5.0E-03 × 69.4 = 0.347 (1.0)	0.114
Mercury			No change (1.0)	0.328
Volatiles				
HNO_3	3.4% (100%)	0.0082 (0.025)	No change (1.0)	0.011
Hydrofluoric acid	No change			0.328
Organics	1.0% (50%)			6.56E-03
Pyrolysis Products				
HCl	N/A			6.56E-03
Phosgene				

a. Original value from Santee (2003) is given in parenthesis.

ARF = airborne release factor
DR = damage ratio
MAR = material at risk
RR = release rate
ST = source term

The following assumptions, however, appear to be more consistent with data from ORNL:

- Escaped gas is composed of off-gas generated from normal operations already resident in the hood
- The bulk of the entrained particulates are from the already-resident gas from normal operations
- In the case of Alternative 1, no additional entrainment of aerosol occurs when the gas escapes during the few-second hood lift.

Investigators from ORNL (1996, p. 27) found hair-like glass fibers up to 91.44 m (300 ft) away from the hood during assessment of their melt expulsion accident. Consequently, this accident scenario may have the potential for greater physical contamination of collocated workers at the distance of 100 m (328 ft) than originally assumed in the FS-PDSA.

6. CONCLUSIONS

Results documented in this EDF identify instances where release fractions differ from those presented in the FS-PDSA, and they are summarized in Tables 1 through 3. In most instances, more detailed analysis of gas generation and release fundamentals has removed some conservatism from the original estimates, and release fractions are considerably lower. In the loss of confinement accident scenario, all contaminant species identified in the FS-PDSA as being at risk of exceeding exposure limits are estimated to be below the limits if the revised exposure factors presented in this EDF are used. In the melt expulsion accident scenario, several species identified by the FS-PDSA to be at risk of exceeding exposure limits (i.e., cadmium, carbon tetrachloride, potassium and sodium nitrates, hydrochloric acid, and phosgene) are estimated to be below the limits if the revised exposure factors are used. However, test data suggest that lead and cesium may be released in greater amounts during the two accident scenarios than originally estimated in the FS-PDSA.

7. RECOMMENDATIONS

The following recommendations are made for future studies of NTISV:

- Obtain better estimates of mass balances for organics and HCl
- Use NTISV test data, when sufficiently plentiful, to estimate destruction and retention efficiencies rather than data from traditional ISV tests
- Consider additional overburden as a means to reduce the LPF
- Further investigate the potential of radioactive contamination for collocated workers during a possible melt expulsion scenario
- Perform waste mapping for potentially problematic waste
- Mitigate potential escape of volatiles to the surrounding ambient soil through additional processing or test to show it does not exist
- Extend methodology and principles used here to other accident scenarios involving the gas-phase release of contaminants.

7.1 Improved Mass Balances

It would be beneficial to have better mass balance estimates for organics and HCl for the ISV process. Geosafe (2001) says 90% of organics are destroyed, and Campbell, Hansen, and Timmerman (1996) says that Geosafe apparently achieved 99% destruction. However, our equilibrium calculations suggest that, without mass transfer and kinetic limitations, some hazardous organics may be generated rather than destroyed. Consequently, organic destruction should be quantitatively confirmed for expected operating conditions and its mechanism should be better understood.

The FS-PDSA assumption that 10% of chlorinated hydrocarbons are converted to HCl was adopted from Reny et al. (1992)[c] and appears to be based on qualitative observations of Torkelson and Rowe (1981). The assumed 10% conversion, however, appears to be much less than that predicted by equilibrium calculations.

Numerical simulation of the mass transfer, kinetics, and thermodynamics associated with pyrolysis and chlorination would be helpful, particularly in support of site-specific areas with high Series 743 organic sludge loadings. Some relevant kinetic data are presented in Appendix A.

7.2 Nontraditional In Situ Vitrification

To be conservative, experimental retention and destruction efficiencies used to modify the release factors were taken from tests of the traditional ISV process. However, one could argue that it would be reasonable and acceptable to use the better efficiencies from test data of the NTISV approach, which has

---

c. Reny, D. A., T. H. Smith, B. M. Meale, T. D. Swantz, T. E. Wierman, T. D. Enyeart, D. J. Strakal, and J. C. Cook, 1992, "Pit 9 Comprehensive Demonstration Preliminary Safety Analysis Report (Draft)," EFF-WM-10186, Idaho National Engineering Laboratory, Appendix F: pp. 31–32.

been identified for ISV processing at the SDA. To do so is advisable if it is determined that enough NTISV data exists on which reliable estimates can be made.

7.3 Better Estimate of LPF_i

The LPF defined by the FS-PDSA was 0.1 for all accident conditions that did not result in disturbances to overburden soils directly on top of ISV melts (typically about 15 cm for conventional ISV processes). Included among these conditions was the loss of confinement scenario, which assumed that the off-gas system would be lost through some undefined accident scenario during ISV processing. Such an accident scenario is not expected to result in any disturbance of the natural soil overburden that is typically above all ISV melts.

The original basis for the 0.1 LPF was data showing a 90% reduction in airborne particulate as gases were passed through a 10-cm (4-in.) thick granular-bed filter (EDF-3563). Such a LPF is appropriate for conventional top-down ISV, where only 15 cm (6 in.) of soil overburden is typically present at all times. However, with NTISV, initiation of the melt is designed to start at depths similar to that at the top of the waste seam, beneath the soil overburden. Such a system is designed to allow the weight of the soil overburden to mitigate concerns associated with rapid gas release events that could result in melt expulsions. According to the DOE standard, "Preparation Guide for U.S. Department of Energy Nonreactor Nuclear Facility Documented Safety Analyses" (DOE-STD-3009-94), unmitigated analyses can ". . .take credit for passive safety features that are assumed to survive accident conditions, where that capability is necessary in order to define a physically meaningful scenario." This means that a safety feature can be accounted for in the unmitigated analysis provided it is not added to the system. Consequently, the impact of the substantially greater soil overburden available with the NTISV process, relative to that of conventional top-down ISV process, can be accounted for in the LPF.

According to Holdren et al. (2002), the soil overburden for the TRU pits (Pits 1-6, 9, and 10) ranges from a minimum thickness of 3–4 ft (Pit 1) to a maximum thickness of 6–9 ft (Pits 4 and 6). For the TRU trenches (Trenches 1–15), the overburden thickness ranges from a minimum of 1.5–3 ft (Trenches 12 and 14) to 2.5–5 ft (Trenches 1, 5, 7, and 9). Such overburden thicknesses (1.5–9 ft) are substantially greater than that typically present in a conventional top-down ISV process. Any additional depth in the overburden should increase the filtration effect, assuming the filtration properties remain the same. However, during excavation for the OU 7-10 Glovebox Excavator Method Project, the overburden was found to be hard packed throughout and broke readily into hard clumps, which might facilitate gas flow to ground surface with subsidence.[d] This suggests that it cannot be assumed that overburden placed years before will stay loose and well divided and provide increased filtration. Consequently, we do not recommend trying to account for preexisting overburden to reduce the LPF lower than 0.1 unless filtration data for cracked, hard-packed soils provides evidence for such reduction.

However, if additional fresh overburden were placed shortly before treatment occurred, remaining loose and finely divided, the filtration capacity could be increased and the LPF reduced. While such a modification is not normally permitted to be included for safety calculations, it could be a simple modification that can be added to the TRU pits and trenches to reduce calculated release rates even further. Additionally, the melt expulsion potential could change from "unlikely" (FS-PDSA) to "extremely unlikely" for an anticipated source term if sufficient overburden were placed on top of the vitrification area before ISV processing.

---

d. Thomas E. Bechtold Personal Communication to Todd T. Nichols, INEEL March 2, 2004 (EDF to be published).

In contrast with the TRU pits and trenches, NTISV processing of the Pad A waste will be performed in staged settings. Therefore, the fresh overburden placed over the preexisting 1 m (3 ft) overburden in these staged settings can be legitimately modified in a manner that reduces the LPF to whatever is needed (as with placement of the waste, to modify material at risk [MAR] factors).

Two possible ways of accounting for fresh overburden in the estimation of a LPF are described below, but Method 2 is recommended.

7.3.1 Potential Revision of Leak Path Factor: Method 1—Extrapolate 10-cm Data

Assuming that the 90% filter efficiency for the previously referenced 10-cm granular bed filter is based on a particle size distribution that offers poor filtration efficiency, the new LPF can be simply multiplied by the difference between the minimal soil overburden (in cm) and 10 cm (to be conservative), and then divided by 10 cm. This is because the behavior of worst-case particle sizes would be cumulative, tending to behave as a series of 10-cm filters. The elimination of one 10-cm filter, made by subtracting the minimal soil overburden thickness by 10 cm, is needed to maintain some conservatism in the calculation. Such conservatism accounts for any disturbance inadvertently created by the system setup, and is consistent with high-efficiency particulate filter bank evaluations.

Unfortunately, it is uncertain (and highly doubtful) that the 90% particle filtration efficiency associated with the 10-cm granular-bed filters is based on a poor particle size distribution. as a result, this method to estimate LPFs probably results in unrealistically low values.

7.3.2 Potential Revision of Leak Path Factor: Method 2—Use Filtration Data Corresponding to Similar Depths

A more prudent method would be to use existing bed filtration data at depths similar to that of the overburden. Data on deep-bed sand filters used at Savannah River Laboratory indicate that sand bed filters with a depth of 2.28 m (7.5 ft) provide a filtration coefficient equivalent to greater than 99.8% (Moyer, Crawford, and Tatum 1975). This corresponds to an LPF_i value less than 0.002 (1 - 0.998). These sand bed filters are typically dry filters arranged in layers with larger diameter particles in the initial layers, shrinking to sand-size particles approximately halfway though the sand filter, with a layer of gravel placed on top of the sand.

The finer particle nature and slight moisture content of soil overburden make the Savannah River Laboratory filtration data conservative for estimating filtration efficiencies. A mathematical function for the LPF can be developed from the two data points at hand (10 cm [4 in.] and 2.28 m [7.5 ft]) that can satisfy the physically limiting values: the LPF has a limiting value of 1 at a depth of zero (no filtration occurs in the complete absence of an overburden), and the function must asymptotically approach zero as the soil depth approaches infinity.

An exponential form ($f(x) = e^{-kx}$) satisfies the limiting values at $x = 0$ and $x = +\infty$, but a value of the adjustable parameter k cannot be found that will adequately predict the LPF values at both $x = 10$ cm and $x = 2.28$ m. This suggests that the soil conditions of the two tests are somewhat dissimilar. An inverse polynomial of second degree was attempted because its form inherently allows exact reproducibility of the two data points, and its form satisfies the limiting values if the constant is given a value of one. The following parameter values satisfy the limiting values and the two data points for the domain $x \geq 0$ of the function $f(x) = 1/(ax^2 + bx + c)$, with the depth x having dimension of meters: $a = 58.68$, $b = 84.13$, and $c = 1.0$.

If only 0.457 m (1.5 ft) of additional soil is placed over the treatment area, the inverse polynomial function above estimates the LPF to be 0.02, a 80% reduction in the LPF relative to the FS-PDSA. This exercise suggests that an LPF much lower than originally assumed in the FS-PDSA could be achieved. It is recommended, in future studies of NTISV processing, that a literature search be performed for additional filtration data to develop a more inclusive correlation for the LPF.

7.4 Radioactive Contamination

Hair-like fibers of glass were found up to 91.44 m (300 ft) away from the hood after the ORNL melt expulsion accident. Therefore, the potential of physical contamination of collocated workers at the distance of 100 m (328 ft) for the melt expulsion accident scenario should be explored further.

7.5 Waste Mapping

Results presented in this EDF do not account for detailed mapping of waste locations in the SDA. Hydrofluoric acid should be removed from the ISV inventory list once the current database information indicating all the hydrofluoric acid is buried only in LLW trenches is validated. It is recommended that disposal locations within the SDA that have substantial quantities of beryllium (soil vault rows and certain trench locations [Holdren et al. 2002]) not be considered for ISV processing.

Gibbs minimization calculations used to estimate destruction and production of various chemical species are sensitive to the presence of oxidation and/or reducing agents (e.g., oxygen, carbon, and hydrogen). More detailed waste mapping would provide a more reliable initial inventory for Gibbs minimization calculations, which would result in an improved estimate of gas composition at elevated temperatures.

As currently stands, the MARs for each contaminant of concern are based on average and calculated bounding hazardous material inventories within the TRU pits and trenches, plus Pad A. However, the batch-like nature of ISV processing, coupled with the heterogeneous concentration of buried waste within the pit, could result in a more varied hazardous material inventory that may, on a site-by-site basis, create areas within the pit where the actual concentration of a specific contaminant exceeds the bounding estimates for that contaminant.

Consequently, it is recommended that waste maps be generated to identify locations where the suspected density of potentially problematic waste is such as to contraindicate application of ISV. Of obvious concern are the potential inventory variation in nitrates, organics, combustibles, cesium, lead, and reaction products (e.g., phosgene and hydrochloric acid). For instance, although the average hazardous material inventory assumed by the FS-PDSA for the ISV treatment area is 1.1×10^6 g for carbon tetrachloride (EDF-3563), a review of the 903-Era Series 743 drum loadings over the ISV treatment area shows that the largest inventory of carbon tetrachloride over a 900-ft^2 area within the SDA may be 4.5×10^7 g (in the northeast corner of Pit 4). This is 40 times that of the average hazardous material inventory assumed in the current evaluation (Miller and Varvel 2001). The peak inventory level of 5×10^7 g is also slightly greater than the reported upper-bound hazardous material inventory of 4.2×10^7 g for carbon tetrachloride used by the FS-PDSA (Santee 2003). Consequently, the release rates for contaminants of concern that can be directly formed from carbon tetrachloride during ISV processing (e.g., phosgene and hydrochloric acid) during actual operations on a location-specific basis may exceed the bounding calculations of the FS-PDSA.

A similar concern involves the extent of mixing between chlorides and cesium. Because of the presence of chlorides in the waste, a higher volatilization of cesium was assumed in this EDF to be conservative. However, accurate waste mapping of cesium and chlorides (e.g., polyvinyl chloride, sodium chloride, potassium chloride, and chlorinated organics) would help to determine whether chlorides and cesium will be within the same treatment area during actual operations.

The staged nature of processing Pad A waste will allow for the ISV process inventory to be modified in a manner that eliminates off-gas emission concerns to both coworkers and the general public.

7.6 Escape of Volatiles to Surrounding Soil

Predictions of the transport model of Jury, Spencer, and Farmer (1983, 1984a, 1984b, 1984c) presented in Appendix B suggest it is possible that the rate of migration of high-Henry's-law-constant species in the ambient zone through gas diffusion could outpace the progression of the melt front. Consequently, in the absence of any test data about transport of volatiles into the surrounding soil, it is recommended that mitigation alternatives be considered. Farnsworth et al. (1999, p. D-8) propose using the vapor vacuum extraction capability currently in place at the SDA or implementing in situ thermal desorption as a pretreatment.

7.7 Other Scenarios

Accident scenarios involving gas release considered by the FS-PDSA but not considered by this EDF include underground fire and drum deflagration. The comments made above about the benefits of improved mass balances and waste mapping, the potential for reducing the LPF value, the appropriateness of using NTISV-specific test data, and the potential of volatiles escaping to the surrounding soil also apply to the underground fire and drum deflagration accident scenarios.

The revised MAR_i and ARF_i values pertaining to normal operations as identified in the discussion of the loss of confinement scenario (see Table 1) can be treated as the baseline values for the underground fire and drum-deflagration scenarios. Adjustments to these factors could then be made as determined by such localized changes as destruction efficiencies and entrainment ratios associated with these accident scenarios.

The underground-fire scenario is expected to be typical of normal operation when the melt front reaches regions of the waste where oxygen from nitrate salts can mix with combustible pyrolysis products from organic waste. as such, high-temperature Gibbs function minimization calculations of pyrolysis and combustion could provide insight into speciation.

It should be noted that the FS-PDSA attaches the large damage ratio factor (i.e., damage ratio = 0.33) to the drum-deflagration event, meaning that 33% of all the waste in the treatment area is affected by the event. This fraction seems extremely high for a localized event involving one drum, and the rationale for using this fraction should be reviewed in future safety analyses.

8. REFERENCES

Aspen, 2001, "ASPEN Plus 11.1," Cambridge, Massachusetts: Aspen Technology.

Buelt, J. L., C. L. Timmerman, K. H. Oma, V. F. FitzPatrick, and J. G. Carter, 1987, *In Situ Vitrification of Transuranic Wastes: An Updated Systems Evaluation And Applications Assessment*, PNL-4800 Supplement 1/UC-70, Pacific Northwest Laboratory.

Campbell, Brett E., James E. Hansen, and Craig L. Timmerman, 1996, *In Situ Vitrification (ISV): An Evaluation of the Disposition of Contaminant Species during Thermal Processing*, Richland, Washington: Geosafe Corporation.

DOE-HDBK-3010-94, 1994, "Airborne Release Fractions/Rates and Respirable Fractions for Nonreactor Nuclear Facilities," Vol. 1, "Analysis of Experimental Data," Change 1, U.S. Department of Energy.

DOE-STD-3009-94, 2002, "Preparation Guide for U.S. Department of Energy Nonreactor Nuclear Facility Documented Safety Analyses," Change Notice No. 2, U.S. Department of Energy.

Dragun, James, 1991, "Geochemistry and Soil Chemistry Reactions Occurring During In Situ Vitrification," *Journal of Hazardous Materials*, Vol. 26, pp. 343–364.

EDF-3543, 2003, "SDA Inventory Evaluation for ISG, ISV, and ISTD PDSA Source Terms," Rev. 0, Idaho National Engineering and Environmental Laboratory.

EDF-3563, 2003, "Radiological Dose and Nonradiological Exposure Calculations for ISV Accident Scenarios," Rev. 0, Idaho National Engineering and Environmental Laboratory.

Farnsworth, R. K., D. M. Henrikson, R. A. Hyde, D. K. Jorgensen, J. K. McDonald, D. F. Nickelson, M. C. Pfeifer, P. A. Sloan, and J. R. Weidner, 1999, *Operable Unit 7-13/14 In Situ Vitrification Treatability Study Work Plan*, DOE/ID-10667, Idaho National Engineering and Environmental Laboratory.

Geosafe, 1998, *Proposal for Performance of a V-Tank In Situ Vitrification Treatability Study*, GSP 02-119711-61 Technical and Cost Proposal, Richland, Washington: Geosafe Corporation.

Geosafe, 2001, "Non-Traditional In Situ Vitrification At The Los Alamos National Laboratory Volume 1 – Hot Demonstration Report," Draft GSC 30101, Columbus, Ohio: Geosafe Corporation.

HAD-268, 2004, "Hazard Assessment for Beryllium Block Grouting at the Radioactive Waste Management Complex," Rev. 0, Idaho National Engineering and Environmental Laboratory.

Holdren, K. Jean, Bruce H. Becker, Nancy L. Hampton, L. Don Koeppen, Swen O. Magnuson, T. J. Meyer, Gail L. Olsen, and A. Jeffrey Sondrup, 2002, *Ancillary Basis for Risk Analysis of the Subsurface Disposal Area*, INEEL/EXT-02-01125, Idaho National Engineering and Environmental Laboratory, September.

Jury, W. A., W. F. Spencer, and W. J. Farmer, 1983, "Behavior Assessment Model for Trace Organics in Soil: I. Model Description," *Journal of Environmental Quality*, Vol. 12, No. 4, October-December, pp. 558–564.

Jury, W. A., W. J. Farmer, and W. F. Spencer, 1984a, "Behavior Assessment Model for Trace Organics in Soil: II. Chemical Classification and Parameter Sensitivity," *Journal of Environmental Quality*, Vol. 13, No. 4, October–December, pp. 567–572.

Jury, W. A., W. F. Spencer, and W. J. Farmer, 1984b, "Behavior Assessment Model for Trace Organics in Soil: III. Applications of Screening Model," *Journal of Environmental Quality*, Vol. 13, No. 4, October–December, pp. 573–579.

Jury, W. A., W. F. Spencer, and W. J. Farmer, 1984c, "Behavior Assessment Model for Trace Organics in Soil: IV. Review of Experimental Evidence," *Journal of Environmental Quality*, Vol. 13, No. 4, October–December, pp. 580–586.

MCP-550, 2003, "Software Management," Rev.7, Idaho National Engineering and Environmental Laboratory.

MCP-2374, 2003, "Analyses and Calculations," Rev. 10, Idaho National Engineering and Environmental Laboratory.

MCP-3039, 2003, "Analysis Software Control," Rev. 4, Idaho National Engineering and Environmental Laboratory.

Miller, Eric C. and Mark D. Varvel, 2001, *Reconstructing the Past Disposal of 743-Series Waste in the Subsurface Disposal Area for Operable Unit 7-08, Organic Contamination in the Vadose Zone,* INEEL/EXT-01-00034, Rev. 0, Idaho National Engineering and Environmental Laboratory, May.

Moyer, R. A., J. H. Crawford, and R. E. Tatum, 1975, "Deep-Bed Sand Filter at Savannah River Laboratory," *Proceedings of the Thirteenth AEC Air Cleaning Conference*, San Francisco, California, August 12–14, 1974, CONF-74087, Vol. 1, National Technical Information Service, U.S. Department of Commerce, Springfield, Virginia.

ORNL, 1996, "Technical Evaluation of the In Situ Vitrification Melt Expulsion at the Oak Ridge National Laboratory, on April 21, 1996," Draft, Oak Ridge National Laboratory.

Outokumpu, 2003, *Outokumpu HSC Chemistry for Windows*, Oy, Finland: Outokumpu Research.

Santee, George E. Jr., 2003, *Feasibility Study Preliminary Documented Safety Analysis for In Situ Vitrification at the Radioactive Waste Management Complex Subsurface Disposal Area*, INEEL/EXT-03-00317, Rev. 0, Idaho National Engineering and Environmental Laboratory.

Torkelson, T. R. and V. K. Rowe, 1981, "Halogenated Aliphatic Hydrocarbons Containing Chlorine, Bromine, and Iodine," In *Patty's Industrial Hygiene and Toxicology*, 3rd Edition, Vol. IIB, New York: John Wiley & Sons.

Zitnik, James F., Aran T. Armstrong, Brian K. Corb, Mark H. Edens, Douglas B. Holsten, Patricia M. O'Flaherty, Janet Rodriquez, Tamara N. Thomas, Russell L. Treat, Wayne Schofield, and Kira L. Sykes, 2002, *Preliminary Evaluation of Remedial Alternatives for the Subsurface Disposal Area*, INEEL/EXT-02-01258, Rev. O, Idaho National Engineering and Environmental Laboratory.

This page is intentionally left blank.

Appendix A

Equilibrium Modeling

This page is intentionally left blank.

Appendix A

Equilibrium Modeling

A-1. PURPOSE

Equilibrium modeling was performed to help envelope possible destruction and retention efficiencies by comparing predictions with experimentally reported values. Gibbs energy minimization routines require the user to input the list of probable species. Consequently, reaction and kinetic data were gathered for key organic and inorganic hazardous species to generate a probable specie list and gain insight to probable residence times for reactions if possible; the smaller the required residence time, the more probable the equilibrium solution.

The common "zone model" (Dragun 1991; Farnsworth et al. 1999) of the physical transport of gas during in situ vitrification (ISV) may not apply at Radioactive Waste Management Complex (RWMC) of the Idaho National Engineering and Environmental Laboratory because of the high number of buried drums relative to the soil volume in the treatment area. Buried conductive inclusions (e.g., drums) appreciably impact temperature profiles (Carey, McLay, and McKinnon 1993), and a simple model of well-defined temperature zones preceding a continuous melt front may not be applicable for the drum-laded conditions of RWMC. Assumptions of the zone model may not be representative of actual field conditions such as the following:

- Water in the soil vaporizes and carries the volatile organics through a well-defined dry zone up to the hood
- Gases homogeneously mix in the dry zone
- Species pyrolyze as they move toward a stable melt front during their journey to the hood.

The equilibrium modeling performed here, therefore, assumes that water and oxygen are not initially present, which tends to reduce the predicted decomposition of organics. Consequently, combustion and hydrolysis reactions were not the primary focus of the literature search; there are many more reactions possible between water, oxygen, and organics than are listed below. However, equilibrium and kinetic simulations of in situ thermal desorption on RWMC waste have been performed (EDF-3699). These simulations offer speciation predictions in the presence of oxygen and water up to temperatures around 760°C.

To be conservative, the lowest of the experimental and equilibrium efficiency was used for each species analyzed in cases where the equilibrium predictions and test data were qualitatively consistent. In cases where the equilibrium predictions differed appreciably from the test data, the test data were presumed to be more representative of actual operations. This assumption is made for several reasons: (1) equilibrium may not be approached in field tests and actual operations because of mass transport or kinetic limitations; (2) the waste inventory is not homogeneously mixed (i.e., not all materials will simultaneously exist in the same treatment area), so many waste components may never come in contact with each other and some reactions may not occur; and (3) the list of potential reactions, and therefore the potential species used in the Gibbs minimization, is not complete. The purpose of the equilibrium modeling was not to supersede appropriate test data, but rather to provide theoretical support to actual data in cases of general agreement.

A-2. KINETICS

Below is a list of some of the reaction/kinetic information available from the literature. Many chlorinated hydrocarbon solvents can react with aluminum, sometimes violently or explosively (Mertens 1993; Holbrook 1993a, 1993b, 1993c), so the aluminum nitrate monohydrate in SDA waste may be a reactant with such hydrocarbons, but potential reactions between hydrocarbons and aluminum compounds were not included in the reaction list below. The specie "benzine" appears in the material lists of EDF-3563, and it is assumed to be a typographical error and that the specie "benzene" was intended. To facilitate information presentation in the form of equations and itemized facts, literature citations are noted by superscript letters. A key relating the superscript letters to references is given at the end of this kinetics section.

Carbon tetrachloride (CCl_4)

CCl_4 = perchloroethylene + hexachloroethane + Cl_2 @400°C:slow, @900–1,300°C:fast . (A-1)[a]

$$CCl_4 + \frac{1}{2}O_2 \xrightarrow{335°C+Iron} COCl_2 + Cl_2$$ 0.375 equil. fraction conversion . (A-2)[a]

$$CCl_4 + 2H_2O \xrightarrow{T\geq 250°C} CO_2 + 4HCl$$ When excess H_2O [a] (A-3a)

(Or view it as the overall reaction[v] composed of the hydrolysis of CCl_4 to $COCl_2$ followed by the faster hydrolysis of $COCl_2$).

$$CCl_4 + H_2O \xrightarrow{T\geq 250°C} COCl_2 + 2HCl$$ k = 30.2 L mol^{-1} min^{-1} @500°C (A-3b)[v]

$k = Ae^{\frac{-E_a}{RT}}$, E_a = 24.95 kcal/mol for 350–450°C

22.05 kcal/mol for 450–550°C

=> A = 5.17E07 L mol^{-1} min^{-1} for 450–550°C

(This is several times slower than hydrolysis of $COCl_2$, so view this step as the H_2O-limited case of the overall reaction above.)

$$2CCl_4 \xrightarrow{T>450°C} \underset{\text{(Tetrachloroethylene)}}{2C_2Cl_4} + 2Cl_2 \ .$$ (A-4)[v]

$$CCl_4 \xrightarrow{400°C+Mercury} \text{Decomposition with liberation of carbon .}$$ (A-5)[a]

CCl_4 + Metallic (Na or K) → explosion . (A-6a)[a]

CCl_4 + Liquid Alloy (Na+K) → explosion . (A-6b)[a]

Chloroform ($CHCl_3$)

$$CHCl_3 + \underset{(Acetone)}{C_3H_6O} \xrightarrow{50°C + AlkaliMetalHydroxide} \underset{\text{(Chloretone: i.e., chlorobutanol or acetone chloroform)}}{C_2Cl_3(CH_3)_2OH} \quad . \qquad \text{(A-7)}^{b}$$

$$CHCl_3 + NO_2 \xrightarrow{270°C} COCl_2 + CO_2 + HCl + H_2O + Others \quad . \qquad \text{(A-8)}^{b}$$

$$CHCl_3 + H_2O \xrightarrow{225°C\,(Prolonged\,Heating)} CO + HCl + \underset{\text{(Formic Acid)}}{CH_2O_2} \quad . \qquad \text{(A-9)}^{b}$$

$$CHCl_3 \xrightarrow{Pyrolysis\,@\,T>450°C} C_2Cl_4 + HCl + \text{Other hydrocarbons in minor amounts} \quad . \qquad \text{(A-10)}^{b}$$

$$CHCl_3 + \frac{1}{2}O_2 \xrightarrow{335°C + Iron} COCl_2 + HCl \qquad \text{0.0024 equil. fraction conversion} \quad . \qquad \text{(A-11)}^{a}$$

Chloroform + hydroxide (i.e., NaOH) can be explosive, especially in the presence of methanol (Holbrook 1993b).

Ethanol (C_2H_5OH)

$$C_2H_5OH + \underset{\text{(Halogen Acid; i.e., HCl, HF)}}{HX} \rightarrow \underset{\text{(Alkyl Halide; i.e., ethyl chloride/fluoride)}}{C_2H_5X} + H_2O \quad . \qquad \text{(A-12)}^{w}$$

$$C_2H_5OH \rightarrow \underset{\text{(Ethylene)}}{C_2H_4} + H_2O \quad . \qquad \text{(A-13)}^{w}$$

Formaldehyde (H_2CO)

$$H_2CO \xrightarrow{400°C} CO + H_2 \qquad \text{decomposition rate = 0.44\%/minute} \quad . \qquad \text{(A-14)}^{k}$$

$$H_2CO + H_2 \xrightarrow{\text{Metal Oxide or Metal}} \underset{\text{(Methanol)}}{CH_4O} \qquad \text{fast} \quad . \qquad \text{(A-15)}^{k}$$

Methylene Chloride (Dichloromethane, CH_2Cl_2)

$$CH_2Cl_2 + H_2O \xrightarrow{Prolonged\,Contact} HCl + Others \quad . \qquad \text{(A-16)}^{f}$$

$$CH_2Cl_2 + H_2O \xrightarrow{Prolonged\,Heating\,@\,140–170°C} \underset{(Formaldehyde)}{H_2CO} + 2HCl \quad . \qquad \text{(A-17)}^{f}$$

$$4CH_2Cl_2 + 4H_2O \xrightarrow{180°C} \underset{(Formic\,Acid)}{CH_2O_2} + 7HCl + \underset{\text{(Methyl Chloride)}}{CH_3Cl} + \underset{(Methanol)}{CH_4O} + CO \quad . \qquad \text{(A-18)}^{f}$$

$$CH_2Cl_2 + NO_2 \xrightarrow{270°C} 2HCl + NO + CO \quad . \qquad \text{(A-19)}^{f}$$

Phosgene ($COCl_2$)

$COCl_{2(liq)} + H_2O_{(liq)} \rightarrow 2HCl + CO_2$ Spontaneous aqueous decomposition (A-20)

slow [c, g]

$r_{COCl2} = k[COCl_2]$, $k = Ae^{\frac{-E_a}{RT}}$, A=1.4E10 s^{-1},
E_a = 53 kJ/mol => k = 7.25 s^{-1} @25°C [h].

$COCl_{2(liq)} + OH^-_{(aq)} \rightarrow HCl + Cl^-_{(aq)} + CO_2$ Hydroxide-induced aqueous decomposition A-(21)

Usual method for removal from waste gases [g]

$r_{COCl2} = k[COCl_2][OH^-]$, k=2.8E4 liter mol^{-1} s^{-1} @25°C [h].

$COCl_{2(g)} + H_2O_{(liq)} = 2HCl + CO_2$ slow: difficult to get intimate mixing of gas and water . (A-22) [c]

$COCl_{2(g)} + H_2O_{(g)} = 2HCl + CO_2$ k=10.07 L mol^{-1} min^{-1} @300°C (A-23) [v]

$k = Ae^{\frac{-E_a}{RT}}$, E_a=12.02 kcal/mol for 220≤ T≤420°C

=> A = 3.86E05 L mol^{-1} min^{-1}

(Is 10^{-35} times greater than hydrolysis of CCl_4) .

$COCl_2 + \underset{(Hydrazine)}{N_2H_4} \rightarrow \underset{(Carbohydrazine)}{NH_2NHCONHNH_2}$ good yields . (A-24) [g]

$COCl_2 + NH_3$ = Urea + Biuret + Ammelide + Cyamelide vigorous . (A-25) [c]

$COCl_2 + \underset{\text{(Alcohols: i.e., Ethyl/Methyl Alchols)}}{ROH} \xrightarrow{\text{High Yields @T≤25° C}} \underset{\text{(Chloroformates: i.e., Ethyl/Methylcarbonate)}}{ROCOCl} + HCl$. (A-26) [u]

$COCl_2$ + Ketones (i.e., methyl isobutyl ketone) → Others + HCl . (A-27) [c, g]

$\underset{(MetalOxide)}{M_xO_y} + zCOCl_2 \xrightarrow{ElevatedTemperature} \underset{(AnhydrousMetalHalide)}{M_xCl_{2y}} + zCO_2$. (A-28) [g]

$COCl_2 + HF \xrightarrow{800°C} \underset{\text{(Carbon Tetrafluoride)}}{CF_4} + CF_3Cl + \underset{\text{(Carbonyl Fluoride)}}{COF_2} + COFCl + Others$. (A-29) [g]

$COCl_2 \rightarrow CO + Cl_2$ Spontaneous gas-phase decomposition (A-30) [d]

50% equil. conversion reached in 60 minutes @470°C

79% equil. conversion reached in 60 minutes @500°C

96% equil. conversion reached in 30 minutes @530°C

99.8% conversion predicted in <7 minutes @700°C.

$COCl_2$ + Hydrogen (from H_2 or hydrocarbons) → CO + 2HCl 100% conv. in 20 minutes @500°C . (A-31) [d]

Potassium Nitrate (KNO_3)

$$KNO_3 \xrightarrow{400°C} \frac{1}{2}K_2O + \frac{1}{2}N_2O_5 \rightarrow \underset{\text{(Potassium Oxide)}}{\frac{1}{2}K_2O} + \underset{\text{(Nitrous Oxide)}}{\frac{1}{2}N_2O} + O_2 \quad . \qquad \text{(A-32)}^{r,s}$$

Potassium oxide begins to decompose @350°C [r].

Potassium nitrate decomposes in a similar fashion as that of sodium nitrate [p].

Sodium Nitrate ($NaNO_3$)

$$NaNO_3 \xrightarrow{380°C} \underset{\text{(Sodium Monoxide)}}{\frac{1}{2}Na_2O} + \underset{\text{(Dinitrogen Pentoxide)}}{\frac{1}{2}N_2O_5} \qquad \text{slow}^{p} \quad . \qquad \text{(A-33)}^{p,r}$$

$$N_2O_5 \xrightarrow{400°C} 2NO_2 + \frac{1}{2}O_2 \qquad \text{immediate: dinitrogen pentoxide is very unstable} \quad . \qquad \text{(A-34)}^{p}$$

$$NaNO_3 \rightarrow \underset{\text{(Sodium Nitrite)}}{NaNO_2} + \frac{1}{2}O_2 \qquad k(\min^{-1}) = 10^{7.33} e^{\frac{-40.3 kcal/mol}{RT}} \quad . \qquad \text{(A-35)}^{n}$$

$$[-\ln(1-\alpha)]^{\frac{1}{3}} = kt$$

@570-760° C

=> α = 0.99 fraction conversion in 36 hours @570°C

α = 0.99 fraction conversion in 26 minutes @760 °C .

$$NaNO_2 \rightarrow \frac{1}{2}Na_2O + \frac{1}{2}N_2 + \frac{3}{4}O_2 \qquad k(\min^{-1}) = 10^{7.67} e^{\frac{-42.8 kcal/mol}{RT}} \quad . \qquad \text{(A-36)}^{n}$$

(Predominant @570–760° C) $[-\ln(1-\alpha)]^{\frac{1}{3}} = kt$

@570-760° C and starting with $NaNO_3$

=> α = 0.99 in 74 hour @570°C

α = 0.99 in 40 minutes @760 °C

Rate is faster in the absence of $NaNO_3$.

$$NaNO_2 \rightarrow \frac{1}{2}Na_2O + NO + \frac{1}{4}O_2$$ Begins @700° C[p] ; minor up to 760° C[n] . (A-37)

$$NaNO_2 + \frac{1}{2}O \rightarrow \frac{1}{2}Na_2O + \frac{1}{2}N_2 + O_2$$ @T ≥ 750° C in the presence of metal catalyst. (A-38)[n]

Produces O and Na_2O_2 (sodium peroxide) as intermediates.

Sodium nitrite begins to decompose @320°C[r] .

Sodium Sulfate (Na_2SO_4)

$Na_2SO_4 \rightarrow Na_2O + SO_3$ slow . (A-39)[p]

Tetrachloroethylene (C_2Cl_4, CCl_2=CCl_2)

$$C_2Cl_4 + 2H_2O \xrightarrow{\text{Prolonged Exposure to Moisture or } T \geq 150°C} \underset{\text{(Trichloroacetic Acid)}}{C_2HCl_3O_2} + HCl \ .$$ (A-40)[q]

$$C_2Cl_4 + O_2 + 2H_2O \rightarrow 2CO_2 + 4HCl \ .$$ (A-41)[p]

$$C_2Cl_4 + Air + Moisture \xrightarrow{\text{Heat}} COCl_2 + HCl + Others \ .$$ (A-42)[q]

$$C_2Cl_4 \xrightarrow{T \geq 500°C}$$ Decomposition w/o air or moisture . (A-43)[q]

$$C_2Cl_4 + \underset{(Formaldehyde)}{H_2CO} + \underset{(Concentrated)}{H_2SO_4} \xrightarrow{80°C}$$ 2,2-Dichloropropanoic acid . (A-44)[q]

$$C_2Cl_4 + \underset{(Metallic)}{K} \xrightarrow{63°C}$$ Explosive reaction . (A-45)[q]

Toluene (C_7H_8)

$$C_7H_8 + O_2 \xrightarrow{50°C} \underset{\text{(Benzoic Acid)}}{C_7H_6O_2} + H_2 \ .$$ (A-46)[x]

$$C_7H_8 + Cl_2 \xrightarrow{100°C} \underset{\text{(Benzyl Chloride}}{C_7H_7Cl} + \underset{\text{(Benzal Chloride)}}{C_7H_6Cl_2} + \underset{\text{(Benzotrichloride)}}{C_7H_5Cl_3} \ .$$ (A-47)[x]

$$2C_7H_8 \rightarrow \underset{\text{(Benzene)}}{C_6H_6} + \underset{\text{(Xylene)}}{C_8H_{10}}$$ (A-48)[x]

1,1,1-Trichloroethane (CH_3CCl_3)

$$CH_3CCl_3 \xrightarrow{325-425°C} \underset{\text{(1,1–Dichloroethylene, Vinylidene Chloride)}}{CH_2CCl_2} + HCl \ .$$ (A-49)[j]

$$\underset{(Dichloroethylene)}{CH_2CCl_2} + \underset{(Concentrated)}{HNO_3} \xrightarrow{Boiled} \underset{\text{(Minor: Chloropicrin)}}{CCl_3NO_2} + Others \ .$$ (A-50)[m]

$$\underset{(Dichloroethylene)}{CH_2CCl_2} + \underset{(Nitrogen\ Peroxide)}{N_2O_4} \xrightarrow{30°C,\ Sealed\ Container} \text{Serious Explosion} \quad . \qquad \text{(A-51)}^{m}$$

Trichloroethylene (C_2HCl_3, $CHCl=CCl_2$)

$$C_2HCl_3 + HNO_3 \xrightarrow{Heat} \text{complete oxidative decomposition} \qquad \text{violent} \quad . \qquad \text{(A-52)}^{e}$$

$$C_2HCl_3 + \underset{(Concentrated)}{HNO_3} \xrightarrow{Boiled} \underset{(Minor:\ Chloropicrin)}{CCl_3NO_2} + \underset{(Major:\ Methylene\ Chloride)}{CH_2Cl_2} \quad . \qquad \text{(A-53)}^{m}$$

$$C_2HCl_3 \rightarrow HCl + \underset{(Dichloroacetylene)}{C_2Cl_2} \qquad \text{Spontaneous gas-phase decomposition @440–460°C} \quad . \qquad \text{(A-54)}^{i}$$

$$r_{C2HCl3} = kP_{C2HCl3,\ Torr},\ k = Ae^{\frac{-E_a}{RT}},\ A = 6.31E13,$$
$$E_a = 56.6\ \text{kcal/mol} \Rightarrow k = 4.9E\text{-}04\ s^{-1}\ @450°C \quad .$$

Chloropicrin (CCl_3NO_2: potential product of 1,1,1-trichloroethane and trichloroethylene decomposition)

$$\underset{(Chloropicrin)}{CCl_3NO_2} \xrightarrow[(99\%\ conv.\ in\ 10\ min.\ @T>300°C)]{150°C} \underset{(Phosgene)}{COCl_2} + NO + Cl_2 + \underset{(minor)}{CCl_4} + \underset{(trace)}{C_2Cl_4} \quad . \qquad \text{(A-55)}^{d}$$

Reference key for equation reference superscript notations are listed below:

a. Holbrook (1993c)
b. Holbrook (1993b)
c. Dunlap (1996)
d. Battin-Leclerc et al. (2000)
e. Mertens (1993)
f. Holbrook (1993a)
g. Babad and Zeiler (1973)
h. Mertens et al. (1994)
i. Kim and Choo (1983)
j. Snedecor (1993)
k. Gerberich and Seaman (1994)
m. Burrows and Hunter (1932)
n. Bond and Jacobs (1966)
p. EDF-3699
q. Hickman (1993)
r. Hawley (1981)
s. Dick (2001)
u. Matzner, Kurkjy, and Cotter (1964)
v. Gaisinovich and Ketov (1969)
w. Logsdon (2003)
x. Ozokwelu (2003).

NOTE: Letters "l," "o," and "t" were not used because of possible confusion with the number one, the number zero, and the dimension time, respectively.

A-3. SIMULATION RESULTS

HSC 5.11 (*Outokumpu HSC Chemistry for Windows*, [Outokumpu 2003]) was the Gibbs minimization software used to estimate equilibrium of the various systems studied. All initial quantities used in the simulations for inorganics are the upper bound (extremely unlikely) values of the MAR_i from the unmitigated melt expulsion accident scenario as given in Santee (2003). The initial quantities for organic species, however, were 100 times the MAR_i because EDF-3563 had reduced the value to one percent of the real inventory due to his assumption of 99% destruction efficiency for organics. The HSC program assumes ideality (i.e., activity coefficient of a specie has the value of one), which should be appropriate for solids and gases, which are the main area of concern—gaseous decomposition products of solids and gas phase chemical equilibrium.

A-3.1. Nitrates

Buelt et al. (1987, pp. xii and 49–50) experimentally determined a minimum destruction efficiency of 96.6% for nitrates with a large-scale test of traditional ISV. Nitrates were assumed to have been effectively reduced to diatomic N_2 and O_2, based on the low quantities of nitrates found in the off-gas scrubber. Equilibrium decomposition for $NaNO_3$ was estimated at temperature intervals of 100° from 100–1,600°C. The following species were included in the model:

- Gases as Phase 1—$NaNO_x$ ($NaNO_2$, $NaNO_3$), N_yO_x (NO, NO_2, N_2O), N_2, and O_2
- Solids or liquids as Phase 2—$NaNO_x$ ($NaNO_3$ and $NaNO_2$)
- Solid as pure phase—Na_2O.

The only initial specie was solid $NaNO_3$. The Na_2O was separated as a pure phase because it is unlikely to be homogeneously mixed with the solid/liquid $NaNO_3$ and $NaNO_2$ because of its much higher melting point. Although N_2O was not a species in the reactions corresponding to sodium nitrate (Equations [A-33]–[A-38]), it was included in the simulation because of similarities between sodium and potassium nitrate (see Equation [A-32]).

The results are presented in Figure A-1, which shows that after the nitrate solids have decomposed ($T \geq 800$°C), the majority of the nitrogen is in the form of diatomic nitrogen, and the nitrate destruction efficiency ranges from 96.8 to 98.8 in the temperature range 800-1,600°C. Consequently, the experimental nitrate destruction efficiency of Buelt et al. (1987) of 96.6 is consistent with the equilibrium estimates and is assumed valid for sodium nitrate. Interestingly, the HSC simulation does not predict significant decomposition until after 700°C even though the literature asserts that decomposition begins as low as 380°C (see Equations [A-16]–[A-23]).

A similar simulation was performed for a hypothetical KNO_3 system. The following species were included (potassium analogs to those included in the sodium nitrate model):

- Gases as Phase 1—KNOx (KNO_2, KNO_3), NyOx (NO, NO_2, N_2O), N_2, and O_2
- Solids or liquids as Phase 2—KNOx (KNO_3 and KNO_2)
- Solid as pure phase—K_2O.

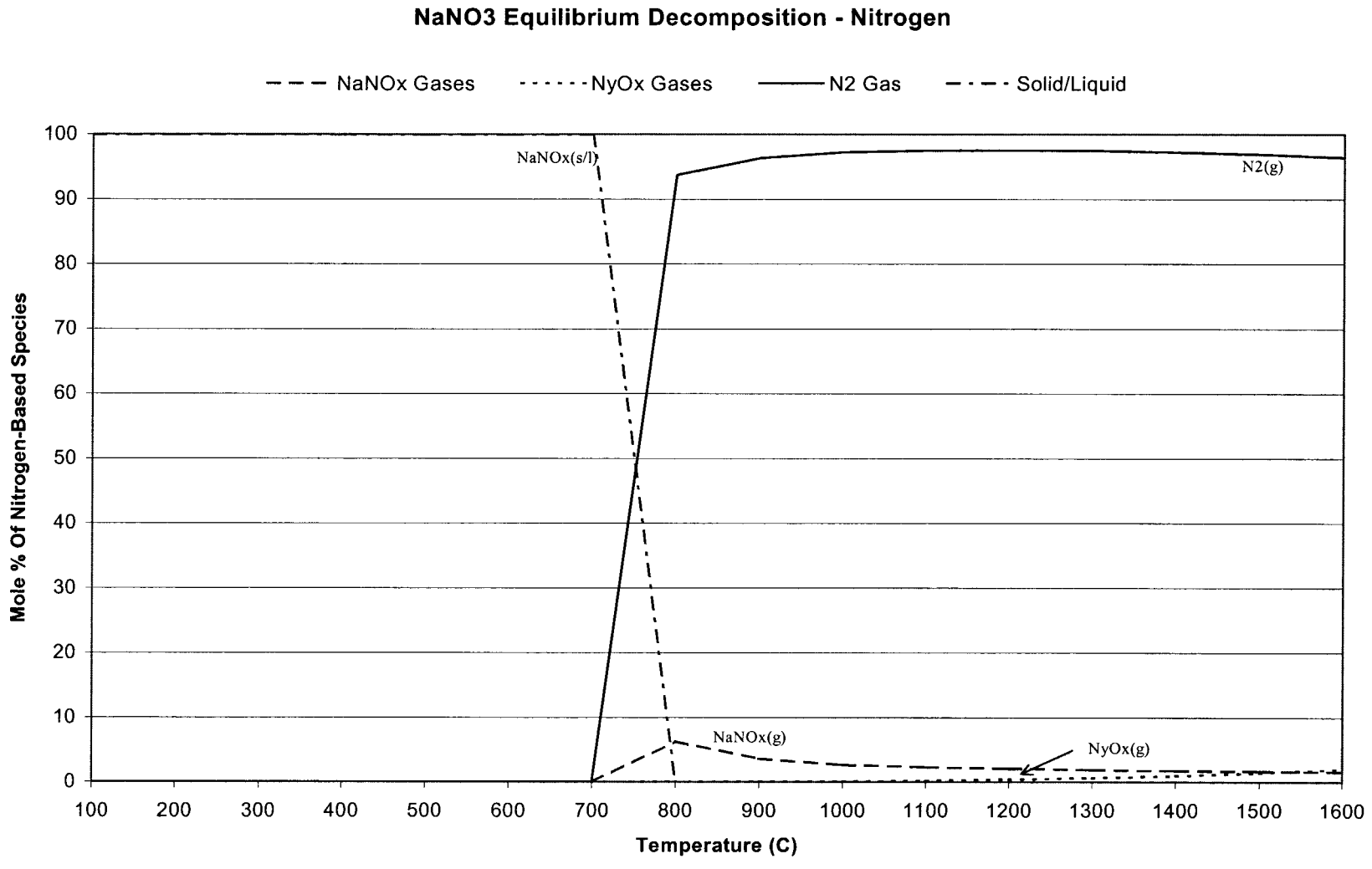

Figure A-1. Predicted $NaNO_3$ equilibrium decomposition.

Because potassium and sodium nitrates decompose in similar manners, the potassium analogs to the sodium-based species included in Equations (A-33)–(A-38) were assumed to be possible species for the decomposition of potassium nitrate. The K_2O was separated as a pure phase because it is unlikely to be homogeneously mixed with the solid or liquid KNO_3 and KNO_2 because of its higher melting point. The results are presented in Figure A-2. A major difference between the results for sodium and potassium is that much of the nitrogen is in the form of alkali metal nitrogen oxides in the case of potassium nitrate ($KNO_{x[g]}$) after the original nitrate solid has decomposed ($T \geq 1{,}100°C$). The nitrate destruction efficiency is appreciably lower for the potassium nitrate, ranging from 54 to 82% over 1,100–1,600°C, with an average of 71%. Consequently, the lower equilibrium-based estimate of 54% nitrate destruction is assumed for potassium nitrate instead of the 96.6% reported by Buelt et al. (1987).

It appears that the destruction efficiency of a solid nitrate in actual ISV operations approaches the equilibrium value, which suggests that the equilibrium concentrations of the decomposition species will be close approximations to reality during actual ISV operations. Figures A-3 and A-4 display the equilibrium diatomic oxygen concentrations predicted for sodium and potassium nitrate, respectively. An appreciable amount of the oxygen content in the original solid nitrate is converted to diatomic oxygen gas, especially in the case of $NaNO_3$. This oxygen, if truly generated, would be available to participate in reactions (e.g., with hydrogen and organics) during its journey to the hood.

The HSC quantitative results of the sodium and potassium nitrate decomposition equilibrations are presented in Tables A-1 and A-2, respectively.

A-3.2. Organics and Acids

Equilibrium concentrations were estimated using HSC at temperature intervals of 100 degrees over the range 100–1600°C of a hypothetical system whose initial constituents are volatile organic and inorganic acid species from the list of hazardous constituents of EDF-3563 as stated previously, the initial quantities for organic species used in the simulation were 100 times the MAR_i of EDF-3563 to account for his assumed organic destruction efficiency of 99%. Nonhazardous materials present in the waste (e.g., iron from steel drums, cellulose from wood, paper, cloth, and cardboard, and polyethylene and polyvinyl chloride from plastic) were not included in the waste constituent tables of EDF-3563. However, many potential organic and inorganic product species not present in the waste were included in the simulation based on the potential reactions from the literature given in the "Kinetics" section.

Figure A-5 displays the concentration profiles for benzene, toluene, xylene, and ethylene. Ethylene was not initially present, but equilibrium favors its creation with increasing temperature. Benzene, although initially present in only a small amount (0.5 kg or 0.022 Kmole), will tend to be formed with increasing temperature. Equilibrium favors the formation of toluene well past its initial presence of 26 kg (1.2 Kmole) below 900°C, and xylene (initially present at 99 kg, or 4.4 Kmole) appears to be favored up to 350°C. The generation of hydrocarbons displayed in Figure A-5 is contrary to the ISV experimental evidence cited by the FS-PDSA to support the assumption of 99% organic destruction efficiency. Perhaps oxygen produced from nitrate decomposition or water contained in the soil contributes to pyrolysis of organics during actual operations. as explained previously, applicable test data are assumed to be more representative of actual ISV operations than are equilibrium predictions; therefore, the 99% organic destruction efficiency used by the Feasibility Study and Preliminary Documented Safety Analysis (FS-PDSA) (Santee 2003) was also used in this engineering design file (EDF).

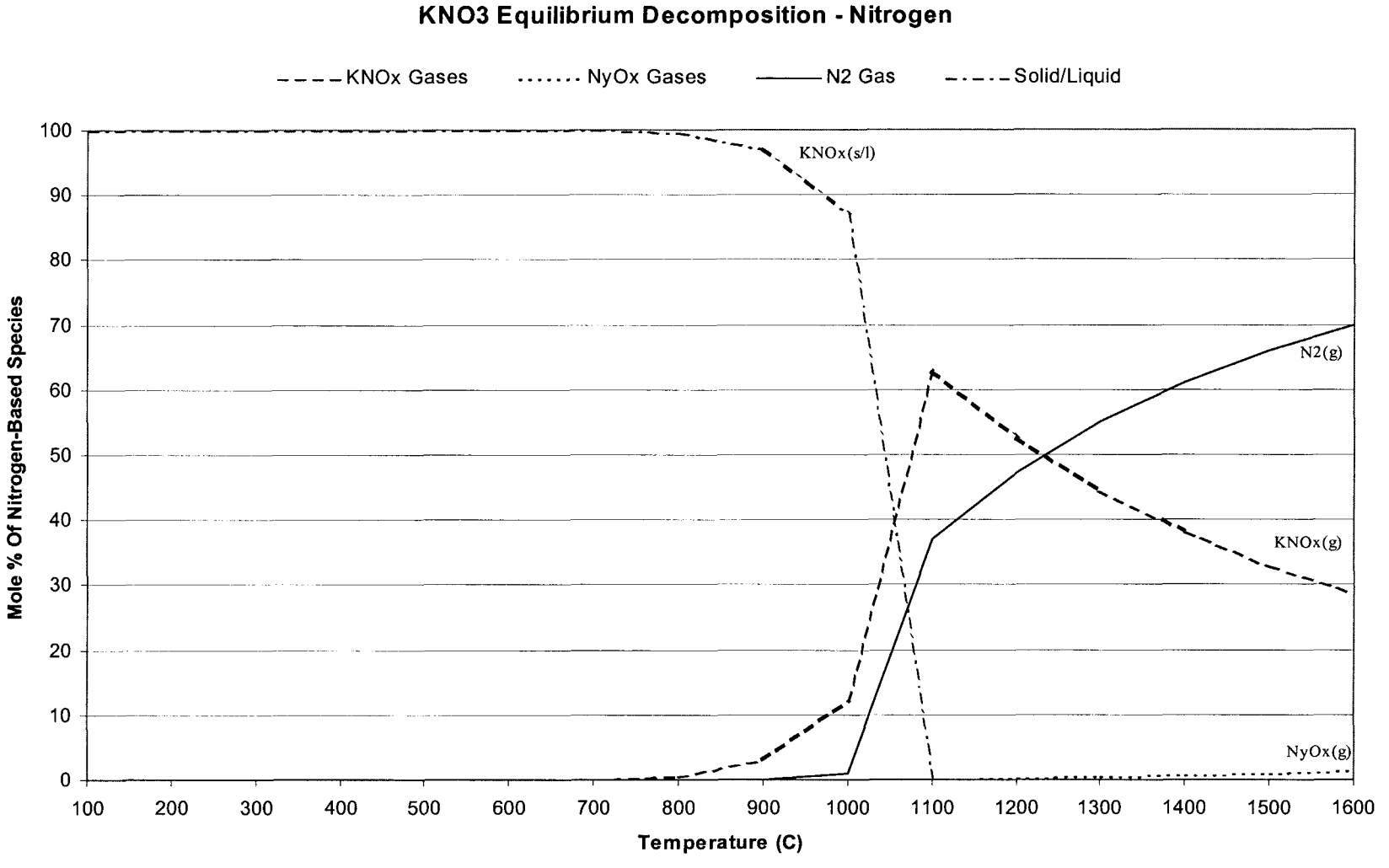

Figure A-2. Predicted KNO_3 equilibrium decomposition.

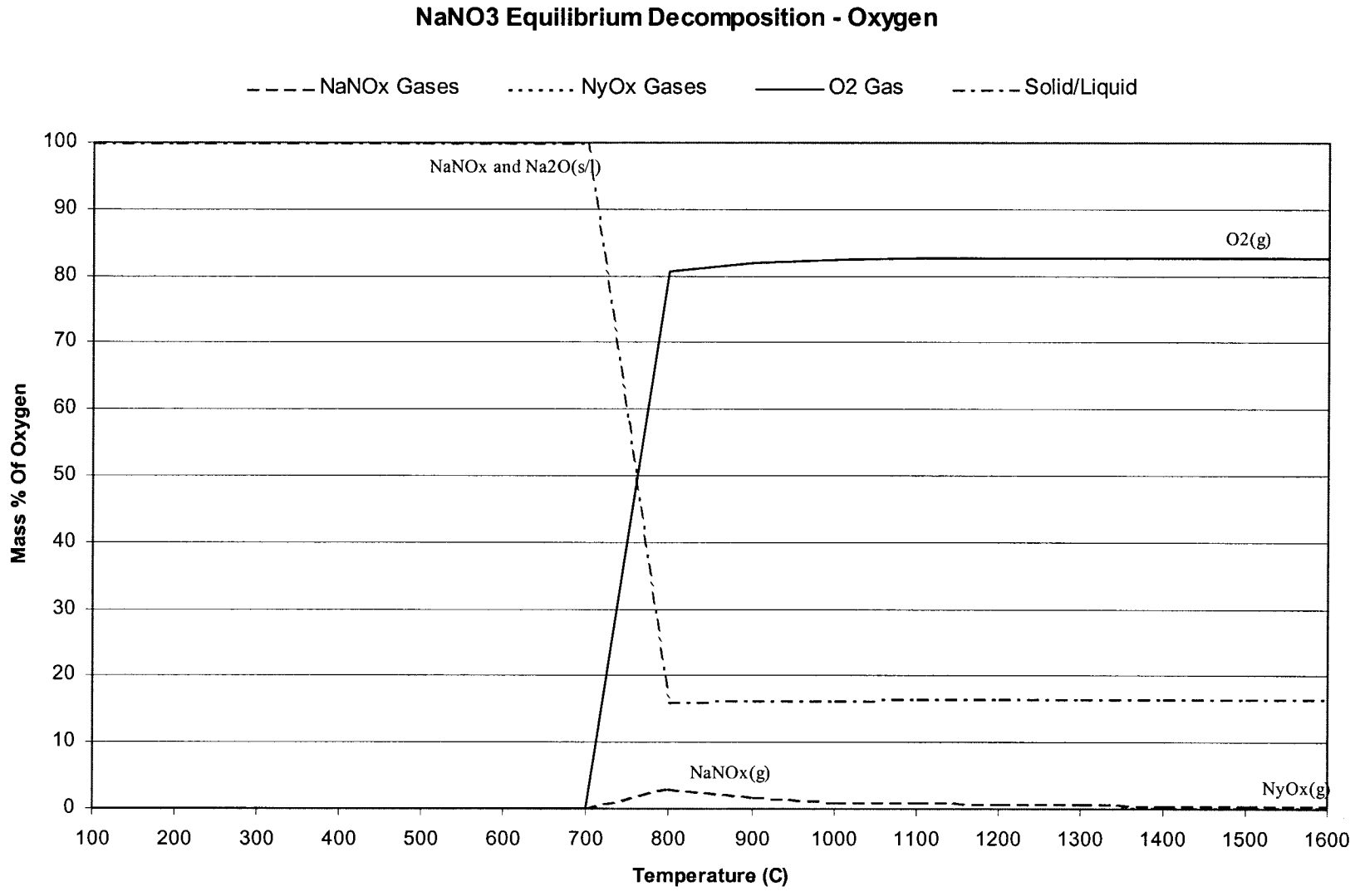

Figure A-3. Predicted equilibrium O_2 generation from $NaNO_3$ decomposition.

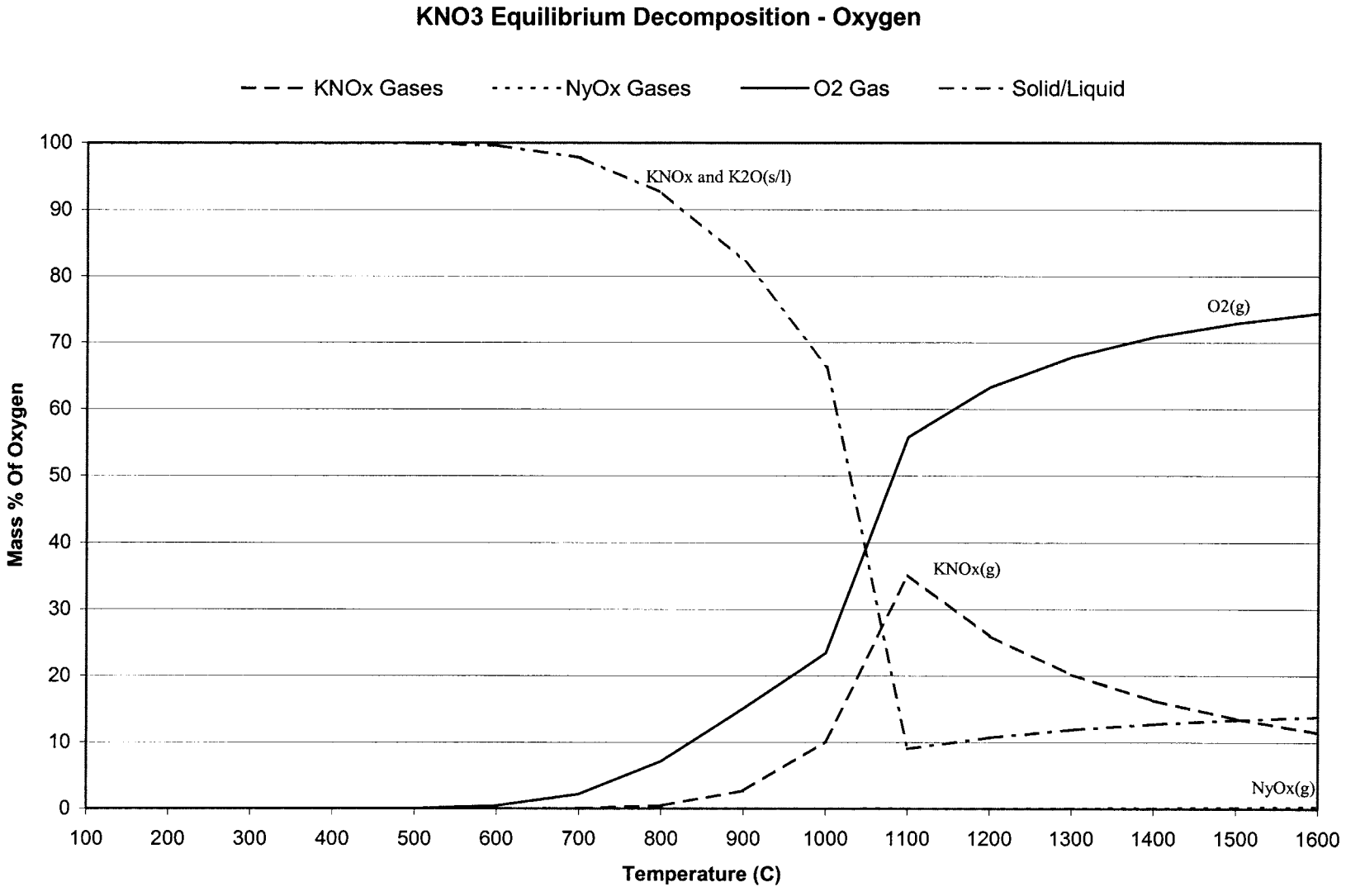

Figure A-4. Predicted equilibrium O_2 generation from KNO_3 decomposition.

Table A-1. HSC results for $NaNO_3$ (Kmoles).

T (C)	1.00E+02	2.00E+02	3.00E+02	4.00E+02	5.00E+02	6.00E+02	7.00E+02	8.00E+02	9.00E+02	1.00E+03	1.10E+03	1.20E+03	1.30E+03	1.40E+03	1.50E+03	1.60E+03
Specie									Kmoles							
O2(g)	1.00E-36	1.00E-36	1.00E-36	1.00E-36	1.00E-36	1.00E-36	3.20E-04	6.84E+03	6.94E+03	6.98E+03	7.00E+03	7.00E+03	7.01E+03	7.01E+03	7.00E+03	7.00E+03
Na2O	1.00E-36	1.00E-36	1.00E-36	1.00E-36	1.00E-36	1.00E-36	1.00E-36	2.73E+03	2.77E+03	2.79E+03	2.79E+03	2.79E+03	2.80E+03	2.80E+03	2.80E+03	2.80E+03
									Nitrogen as Solid/Liquid							
NaNO3	5.65E+03	5.65E+03	5.65E+03	5.65E+03	5.65E+03	5.65E+03	5.65E+03	1.00E-36	1.00E-36	1.00E-36	1.00E-36	1.00E-36	1.00E-36	1.00E-36	1.00E-36	1.00E-36
NaNO2	2.06E-13	3.71E-10	5.55E-08	1.79E-06	2.18E-05	1.43E-04	6.23E-04	1.00E-36	1.00E-36	1.00E-36	1.00E-36	1.00E-36	1.00E-36	1.00E-36	1.00E-36	1.00E-36
									Nitrogen as Gas Other Than N2							
NaNO2(g)	1.00E-36	1.00E-36	1.00E-36	1.00E-36	1.00E-36	1.00E-36	1.22E-07	2.22E+01	3.09E+01	3.96E+01	4.69E+01	4.90E+01	4.84E+01	4.74E+01	4.63E+01	4.50E+01
NaNO3(g)	1.00E-36	1.00E-36	1.00E-36	1.00E-36	1.00E-36	1.00E-36	4.07E-06	1.60E+02	7.23E+01	3.59E+01	1.90E+01	9.90E+00	5.34E+00	3.08E+00	1.88E+00	1.21E+00
NO(g)	1.00E-36	1.00E-36	1.00E-36	1.00E-36	1.00E-36	1.00E-36	1.85E-09	7.02E-01	1.71E+00	3.58E+00	6.73E+00	1.16E+01	1.87E+01	2.83E+01	4.10E+01	5.71E+01
NO2(g)	1.00E-36	1.00E-36	1.00E-36	1.00E-36	1.00E-36	1.00E-36	2.62E-10	4.33E-02	6.09E-02	8.05E-02	1.02E-01	1.25E-01	1.50E-01	1.76E-01	2.02E-01	2.30E-01
N2O(g)	1.00E-36	1.00E-36	1.00E-36	1.00E-36	1.00E-36	1.00E-36	1.78E-14	3.23E-05	7.31E-05	1.45E-04	2.60E-04	4.32E-04	6.75E-04	1.00E-03	1.42E-03	1.95E-03
									Nitrogen as Diatomic N2 Gas							
N2(g)	1.00E-36	1.00E-36	1.00E-36	1.00E-36	1.00E-36	1.00E-36	3.33E-06	2.73E+03	2.77E+03	2.78E+03	2.79E+03	2.79E+03	2.79E+03	2.78E+03	2.78E+03	2.77E+03

Table A-2. HSC results for KNO_3 (Kmoles).

T (C)	1.00E+02	2.00E+02	3.00E+02	4.00E+02	5.00E+02	6.00E+02	7.00E+02	8.00E+02	9.00E+02	1.00E+03	1.10E+03	1.20E+03	1.30E+03	1.40E+03	1.50E+03	1.60E+03
Specie									Kmoles							
O2(g)	1.00E-36	1.00E-36	3.47E-03	1.20E-01	1.77E+00	1.52E+01	7.78E+01	2.54E+02	5.39E+02	8.35E+02	1.99E+03	2.25E+03	2.42E+03	2.52E+03	2.60E+03	2.65E+03
K2O	1.00E-36	1.00E-36	1.00E-36	1.00E-36	1.00E-36	1.00E-36	1.00E-36	7.15E-04	2.32E-01	2.21E+01	6.44E+02	7.63E+02	8.46E+02	9.06E+02	9.51E+02	9.86E+02
									Nitrogen as Solid/Liquid							
KNO3	2.37E+03	2.37E+03	2.37E+03	2.37E+03	2.37E+03	2.34E+03	2.22E+03	1.85E+03	1.24E+03	6.15E+02	1.00E-36	1.00E-36	1.00E-36	1.00E-36	1.00E-36	1.00E-36
KNO2	5.66E-09	3.03E-05	6.93E-03	2.39E-01	3.54E+00	3.04E+01	1.56E+02	5.08E+02	1.06E+03	1.43E+03	1.00E-36	1.00E-36	1.00E-36	1.00E-36	1.00E-36	1.00E-36
									Nitrogen as Gas Other Than N2							
KNO2(g)	1.00E-36	1.00E-36	5.45E-17	1.12E-11	8.42E-08	8.03E-05	1.57E-02	8.60E-01	1.55E+01	1.31E+02	7.56E+02	6.93E+02	6.07E+02	5.24E+02	4.51E+02	3.90E+02
KNO3(g)	1.00E-36	1.00E-36	1.14E-10	4.90E-07	2.11E-04	2.23E-02	7.60E-01	9.96E+00	5.38E+01	1.54E+02	3.30E+02	1.54E+02	7.41E+01	3.75E+01	2.01E+01	1.14E+01
NO(g)	1.00E-36	1.00E-36	3.95E-14	4.11E-12	1.36E-10	1.34E-09	2.96E-07	6.75E-05	4.33E-03	1.10E-01	1.72E+00	3.44E+00	6.03E+00	9.68E+00	1.46E+01	2.08E+01
NO2(g)	1.00E-36	1.00E-36	8.55E-13	1.45E-11	1.25E-10	4.36E-10	4.22E-08	4.86E-06	1.73E-04	2.51E-03	2.27E-02	3.37E-02	4.50E-02	5.66E-02	6.85E-02	8.06E-02
N2O(g)	1.00E-36	1.00E-36	4.57E-21	6.10E-20	4.39E-19	8.21E-19	1.89E-15	9.38E-12	6.77E-09	1.16E-06	5.20E-05	1.07E-04	1.90E-04	3.06E-04	4.61E-04	6.60E-04
									Nitrogen as Diatomic N2 Gas							
N2(g)	1.00E-36	1.00E-36	9.84E-10	1.04E-09	1.13E-09	4.88E-10	3.51E-07	6.79E-04	2.29E-01	2.20E+01	6.43E+02	7.62E+02	8.43E+02	9.01E+02	9.44E+02	9.76E+02

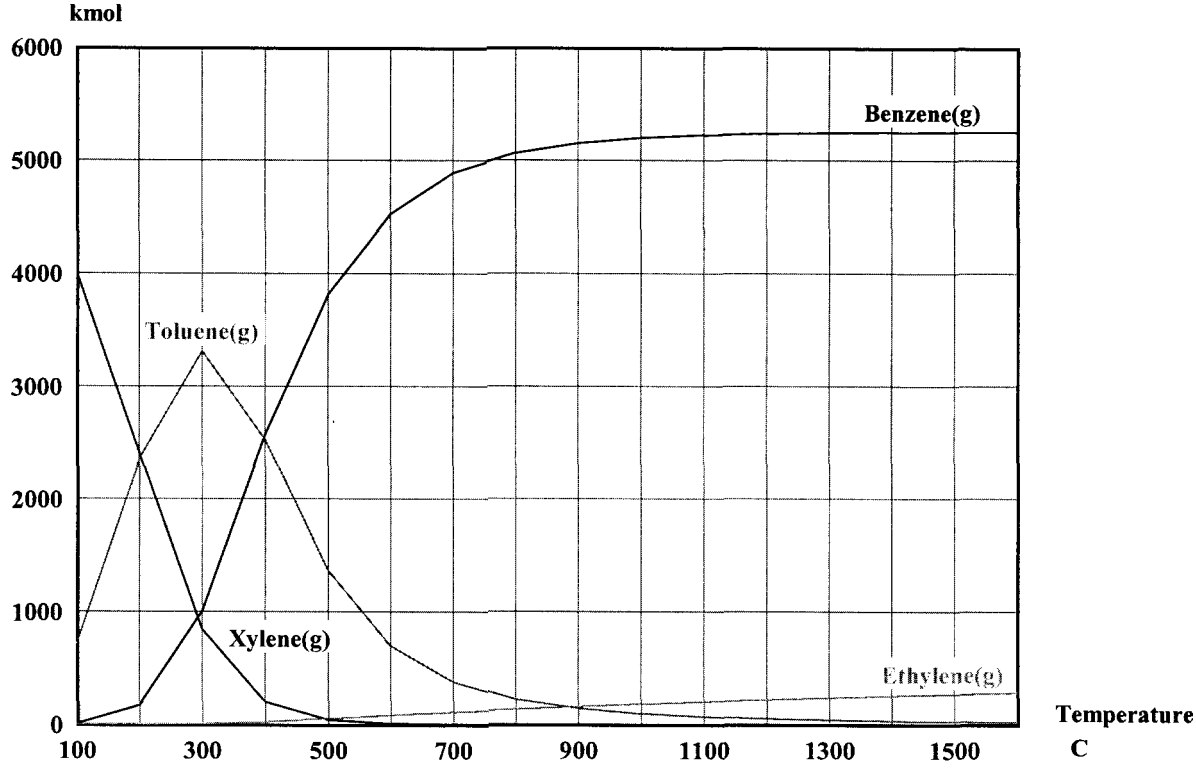

Figure A-5. Predicted organic gases.

The FS-PDSA assumes that 10% of the chlorinated hydrocarbons decompose to HCl, and that 1% of all chlorinated compounds decompose to phosgene with a molecular conversion ratio of 1.19. Summing the chlorinated hydrocarbons (1,1,1-trichloroethane, methylene chloride, trichloroethylene, and chloroform) results in 1,227 Kmoles, giving 123 Kmoles of HCl (1,227 × 0.1). The predicted equilibrium conversion to HCl is displayed in Figure A-6 and has the value of 13,000 Kmoles, which is considerably higher than the assumed 10% conversion. The equilibrium conversion is obviously an upper bound because not all the materials are expected to simultaneously exist in the same treatment area.

Summing the chlorinated compounds (the chlorinated hydrocarbons, 1,1,2-trichloro-1,2,2-trifluoroethane, tetrachloroethylene, and carbon tetrachloride) results in 3,587 Kmoles, giving 43 Kmoles of phosgene assuming a conversion of 1.19% (3,587 × 0.0119). The predicted equilibrium conversion of phosgene vs. temperature is displayed in Figure A-7. The highest amount predicted is on the order of 10^{-7} Kmoles and corresponds to 1,600°C. Consequently, the assumed conversion of 0.0119 appears to be conservative (high) relative to Gibbs minimization calculations.

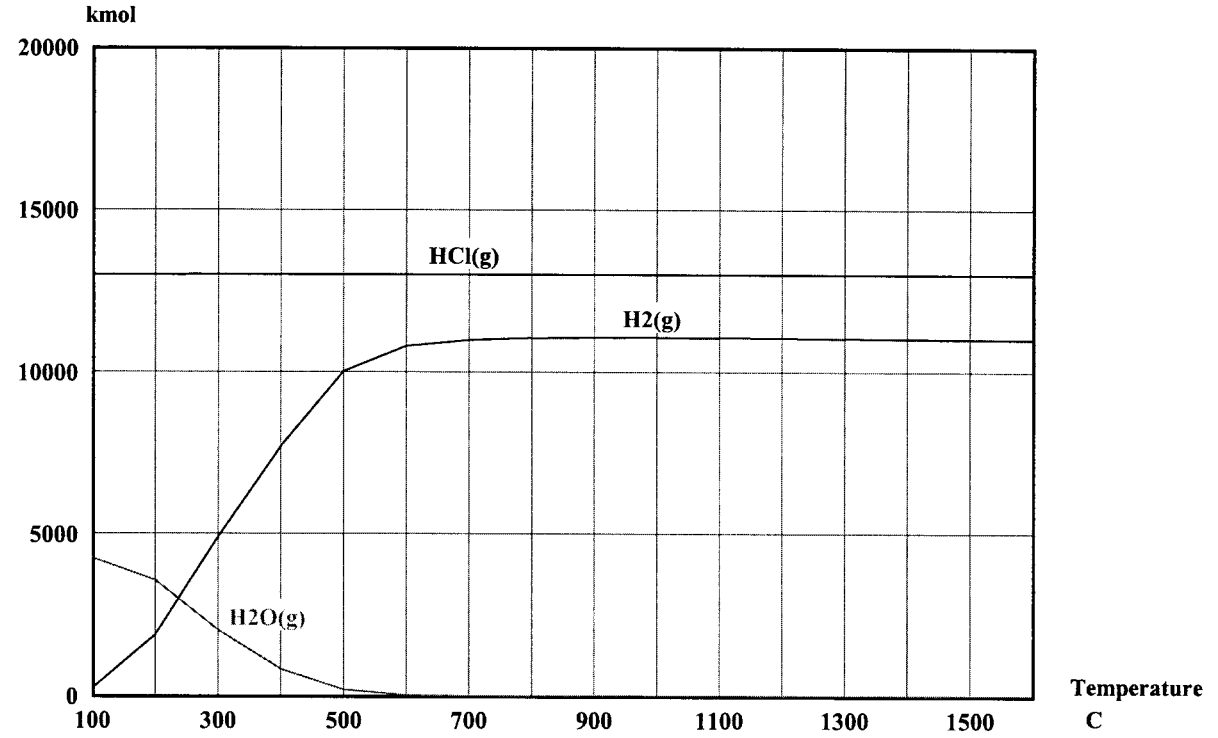

Figure A-6. Predicted hydrochloric acid, hydrogen, and water generation.

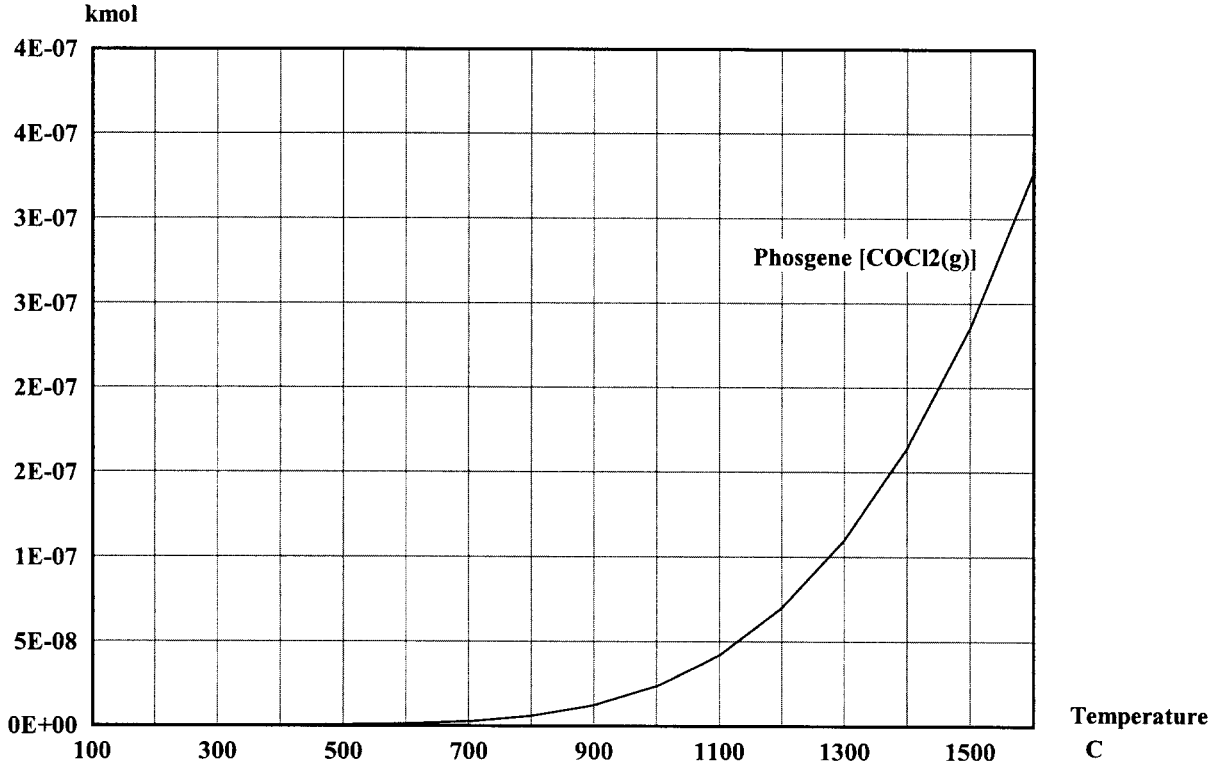

Figure A-7. Predicted phosgene generation.

The history of the FS-PDSA assumption of 10% conversion to HCl and 1% conversion to phosgene is interesting. The source cited by the FS-PDSA is an earlier document (EDF-3563), that in turn cites Slaughterbeck et al. (1995) (Chapter 7, pp. 15–16), which cites the "Pit 9 Comprehensive Demonstration Preliminary Safety Analysis Report (Draft),"[a] which in turn references Torkelson and Rowe (1981). This last reference is a 170-page chapter in a three-volume book, and we could not find a citation for phosgene in the index corresponding to that chapter of that volume. The draft Preliminary Safety Analysis Report (see footnote a) states the following:

> The chlorinated hydrocarbons are nonflammable and will vaporize when exposed to fire. However, when exposed to heat and fire, all halogenated compounds can be broken down to produce halogenated acids and in some cases much smaller concentrations of phosgene-type compounds. Except for very unusual circumstances, phosgene concentrations have been shown to be much lower than the acids (references Torkelson and Rowe [1981]). Because of their resistance to fire (carbon tetrachloride was formerly used in fire extinguishers) and the volume of the processing facility for expansion of vapors, it is assumed that at least 89% of the chlorinated hydrocarbons will volatilize. Of the remaining 11%, it is conservatively assumed that 10% decompose to HCl and 1% decompose to phosgene gas.

The original source of the HCl/phosgene conversion assumption appears to be from the Draft Pit 9 Preliminary Safety Analysis Report (see footnote a), and it appears to have some basis in a qualitative observation from Torkelson and Rowe (1981). These assumed conversions of HCl and phosgene, although not consistent with equilibrium calculations, are used in this EDF because of the previously explained deference to test data.

Buelt et al. (1987, pp. xii and 49) experimentally determined a retention efficiency of 98.8% for fluorides with traditional ISV, but a description of the form of the fluorides included in the waste was not given. The equilibrium calculations, however, suggest that hydrofluoric acid in INEEL waste is generated rather than consumed. Forty-four Kmoles are initially present, but thermodynamic equilibrium would correspond to a final amount of 177 Kmoles. Perhaps hydrofluoric acid would be trapped in the melt through solubility or binding during actual operations. However, because of the uncertain applicability of the test data, it is conservatively assumed that all the hydrofluoric acid initially present reaches the off-gas hood.

Buelt et al. (1987, pp. xii and 49–50) experimentally determined a minimum destruction efficiency of 96.6% for nitrates with a large-scale test of traditional ISV, and the equilibrium calculation predicts that all the nitric acid is consumed, supporting the experimental finding for the specie HNO_3.

The initial amounts for the HSC simulation are listed in Table A-3, and the quantitative results in Kmoles are presented in Table A-4.

---

a. Reny, D. A., T. H. Smith, B. M. Meale, T. D. Swantz, T. E. Wierman, T. D. Enyeart, D. J. Strakal, and J. C. Cook, 1992, "Pit 9 Comprehensive Demonstration Preliminary Safety Analysis Report (Draft)," EFF-WM-10186, Idaho National Engineering Laboratory, Appendix F: pp. 31–32.

Table A-3. Inputs for Gibbs minimization of organics and acids.

Compound Name		Initial Amount	
FS-PDSA[a]	HSC 5.11	kg	Kmole
1,1,2-Trichloro-1,2,2-Trifluoroethane	$C_2Cl_3F_3$(112TCFg)	990	44.17
Tetrachloroethylene	C_2Cl_4(g)	9,900	441.696
Vinylidene chloride	$C_2H_2Cl_2$(11DCEg)	—	—
1,1,1-Trichloroethane	$C_2H_3Cl_3$(g)	13,000	580.005
Methyl chloroformate	$C_2H_3ClO_2$(MCFg)	—	—
Ethylene	C_2H_4(g)	—	—
Ethyl chloride	C_2H_5Cl(CEAg)	—	—
Ethyl fluoride	C_2H_5F(EFLg)	—	—
Ethyl alcohol	C_2H_6O(EAOg)	290	12.939
Trichloroethylene	C_2HCl_3(g)	13,000	580.005
Ethyly chloroformate	$C_3H_5ClO_2$(ECFg)	—	—
Acetone	C_3H_6O(PREg)	14	0.625
Butyl alcohol	$C_4H_{10}O$(BUTg)	1,200	53.539
Methyl isobutyl ketone	$C_6H_{12}O$(4M2PNg)	120,000	5,353.892
Benzine (assumed Benzene was meant)	C_6H_6(BZEg)	0.5	0.022
Benztrichloride	$C_7H_5Cl_3$(BTCg)	—	—
Benzoic acid	$C_7H_6O_2$(BAg)	—	—
Benzyl chloride	C_7H_7Cl(BYCg)	—	—
Toluene	C_7H_8(TLUg)	26	1.16
Xylene	C_8H_{10}(PXYg)	99	4.417
Carbon tetrachloride	CCl_4(g)	42,000	1,873.862
Chlorotrifluoromethane	$CClF_3$(g)	—	—
Carbon tetrafluoride	CF_4(g)	—	—
Methylene chloride	CH_2Cl_2(g)	1,500	66.924
Formaldehyde	CH_2O(g)	1,500	66.924
Methyl chloride	CH_3Cl(g)	—	—
Methyl alcohol	CH_3OH(g)	2,600	116.001
Chloroform	$CHCl_3$(g)	0.0038	0
Chlorine	C_{l2}(g)	—	—
Carbon monoxide	CO(g)	—	—
Carbon dioxide	CO_2(g)	—	—

Table A-3. (continued).

Compound Name		Initial Amount	
FS-PDSA[a]	HSC 5.11	kg	Kmole
Phosgene	$COCl_2(g)$	—	—
Carbonyl fluoride	$COF_2(g)$	—	—
Hydrogen	$H_2(g)$	—	—
Water	$H_2O(g)$	—	—
Hydrogen chloride	$HCl(g)$	—	—
Formic acid	$HCOOH(g)$	—	—
Hydrofluoric acid	$HF(g)$	990	44.17
Nitric acid	$HNO_3(g)$	63	2.811
Hydrazine	$N_2H_4(g)$	0.23	0.01
Nitrogen peroxide	$N_2O_4(g)$	—	—
Ammonia	$NH_3(g)$	190	8.477
Nitric oxide	$NO(g)$	—	—
Nitrogen dioxide	$NO_2(g)$	—	—
Oxygen	$O_2(g)$	—	—

a. Name used by the FS-PDSA (Santee 2003) for those species present in the waste inventory.

Table A-4. HSC results for organics and acids (Kmoles).

T (C)	100	200	300	400	500	600	700	800	900	1,000	1,100	1,200	1,300	1,400	1,500	1,600
Species	Kmoles															
C2Cl3F3(112TCFg)	1.00E-36	1.00E-36	1.00E-36	1.00E-36	1.00E-36	1.00E-36	3.09E-35	3.22E-33	1.59E-31	4.38E-30	7.64E-29	9.20E-28	8.20E-27	5.69E-26	3.20E-25	1.51E-24
C2Cl4(g)	1.00E-36	3.23E-36	9.07E-31	1.18E-26	1.59E-23	6.15E-21	8.13E-19	4.50E-17	1.29E-15	2.20E-14	2.52E-13	2.09E-12	1.33E-11	6.82E-11	2.92E-10	1.07E-09
C2H2Cl2(11DCEg)	1.24E-20	2.26E-16	1.96E-13	2.61E-11	9.65E-10	1.75E-08	1.83E-07	1.24E-06	6.11E-06	2.35E-05	7.48E-05	2.03E-04	4.88E-04	1.06E-03	2.09E-03	3.85E-03
C2H3Cl3(g)	1.22E-21	5.79E-19	4.47E-17	1.07E-15	1.09E-14	7.76E-14	3.98E-13	1.54E-12	4.79E-12	1.26E-11	2.91E-11	6.03E-11	1.15E-10	2.03E-10	3.39E-10	5.38E-10
C2H3ClO2(MCFg)	7.74E-17	1.23E-14	3.15E-13	1.71E-12	1.35E-12	2.63E-13	5.66E-14	1.63E-14	5.92E-15	2.57E-15	1.28E-15	7.06E-16	4.25E-16	2.74E-16	1.86E-16	1.32E-16
C2H4(g)	4.85E-03	4.92E-01	5.88E+00	2.32E+01	5.19E+01	8.15E+01	1.09E+02	1.35E+02	1.58E+02	1.80E+02	2.00E+02	2.19E+02	2.36E+02	2.52E+02	2.66E+02	2.80E+02
C2H5Cl(CEAg)	5.57E+00	3.64E+00	1.52E+00	5.43E-01	1.99E-01	8.19E-02	3.89E-02	2.09E-02	1.24E-02	8.02E-03	5.52E-03	4.00E-03	3.03E-03	2.37E-03	1.90E-03	1.56E-03
C2H5F(EFLg)	3.80E-06	2.08E-05	3.42E-05	3.20E-05	2.39E-05	1.70E-05	1.24E-05	9.49E-06	7.55E-06	6.21E-06	5.26E-06	4.56E-06	4.04E-06	3.64E-06	3.32E-06	3.07E-06
C2H6O(EAOg)	4.79E-04	1.63E-03	1.27E-03	4.30E-04	6.86E-05	6.27E-06	7.59E-07	1.32E-07	3.06E-08	8.93E-09	3.12E-09	1.26E-09	5.76E-10	2.90E-10	1.58E-10	9.25E-11
C2HCl3(g)	8.67E-30	2.68E-24	2.31E-20	2.00E-17	3.29E-15	2.17E-13	6.67E-12	1.11E-10	1.16E-09	8.43E-09	4.63E-08	2.03E-07	7.38E-07	2.31E-06	6.37E-06	1.58E-05
C3H5ClO2(ECFg)	1.04E-15	2.55E-14	1.40E-13	2.07E-13	5.48E-14	4.31E-15	4.41E-16	6.85E-17	1.49E-17	4.17E-18	1.43E-18	5.78E-19	2.65E-19	1.35E-19	7.45E-20	4.40E-20
C3H6O(PREg)	2.29E-02	6.27E-02	5.27E-02	2.03E-02	3.56E-03	3.59E-04	4.72E-05	8.77E-06	2.15E-06	6.58E-07	2.40E-07	1.00E-07	4.70E-08	2.42E-08	1.34E-08	7.96E-09
C4H10O(BUTg)	5.92E-05	3.58E-05	5.21E-06	3.69E-07	1.47E-08	4.15E-10	1.91E-11	1.50E-12	1.80E-13	3.01E-14	6.56E-15	1.77E-15	5.69E-16	2.11E-16	8.80E-17	4.06E-17
C6H12O(4M2PNg)	1.03E-02	9.99E-04	3.25E-05	5.53E-07	5.33E-09	3.89E-11	4.88E-13	1.09E-14	3.86E-16	1.98E-17	1.37E-18	1.21E-19	1.31E-20	1.68E-21	2.50E-22	4.20E-23
C6H6(BZEg)	9.11E+00	1.71E+02	1.01E+03	2.57E+03	3.81E+03	4.53E+03	4.89E+03	5.06E+03	5.15E+03	5.20E+03	5.22E+03	5.24E+03	5.24E+03	5.25E+03	5.25E+03	5.25E+03
C7H5Cl3(BTCg)	3.38E-27	6.44E-23	1.01E-19	2.32E-17	1.17E-15	3.07E-14	4.51E-13	4.09E-12	2.58E-11	1.24E-10	4.74E-10	1.52E-09	4.19E-09	1.02E-08	2.23E-08	4.42E-08
C7H6O2(BAg)	4.35E-10	4.00E-08	7.57E-07	2.80E-06	1.33E-06	1.58E-07	2.15E-08	4.07E-09	1.02E-09	3.13E-10	1.14E-10	4.68E-11	2.13E-11	1.05E-11	5.43E-12	2.94E-12
C7H7Cl(BYCg)	1.45E-05	2.13E-04	8.13E-04	1.18E-03	8.86E-04	5.64E-04	3.33E-04	1.90E-04	1.08E-04	6.22E-05	3.65E-05	2.19E-05	1.35E-05	8.49E-06	5.45E-06	3.56E-06
C7H8(TLUg)	7.21E+02	2.35E+03	3.31E+03	2.53E+03	1.36E+03	6.98E+02	3.79E+02	2.23E+02	1.41E+02	9.55E+01	6.82E+01	5.10E+01	3.95E+01	3.16E+01	2.59E+01	2.15E+01
C8H10(PXYg)	4.00E+03	2.41E+03	8.43E+02	1.98E+02	3.97E+01	9.01E+00	2.52E+00	8.54E-01	3.43E-01	1.57E-01	8.06E-02	4.52E-02	2.74E-02	1.76E-02	1.20E-02	8.48E-03
CCl4(g)	1.00E-36	1.00E-31	1.50E-27	2.27E-24	6.15E-22	6.70E-20	3.21E-18	7.78E-17	1.12E-15	1.08E-14	7.54E-14	4.08E-13	1.80E-12	6.65E-12	2.13E-11	6.05E-11
CClF3(g)	1.48E-32	5.93E-29	3.61E-26	5.59E-24	2.76E-22	8.04E-21	1.35E-19	1.39E-18	9.86E-18	5.23E-17	2.20E-16	7.71E-16	2.32E-15	6.16E-15	1.47E-14	3.23E-14
CF4(g)	8.83E-29	1.64E-26	1.33E-24	4.92E-23	8.38E-22	1.07E-20	9.29E-20	5.62E-19	2.56E-18	9.34E-18	2.86E-17	7.61E-17	1.80E-16	3.88E-16	7.69E-16	1.43E-15
CH2Cl2(g)	2.60E-11	2.31E-09	4.90E-08	4.35E-07	2.13E-06	7.86E-06	2.28E-05	5.47E-05	1.13E-04	2.10E-04	3.58E-04	5.67E-04	8.50E-04	1.22E-03	1.67E-03	2.23E-03
CH2O(g)	9.86E-11	1.65E-07	1.60E-05	2.61E-04	9.34E-04	1.08E-03	1.02E-03	9.63E-04	9.13E-04	8.72E-04	8.39E-04	8.13E-04	7.92E-04	7.76E-04	7.63E-04	7.53E-04
CH3Cl(g)	5.28E-01	1.65E+00	2.51E+00	2.71E+00	2.53E+00	2.25E+00	2.00E+00	1.80E+00	1.64E+00	1.51E+00	1.41E+00	1.32E+00	1.25E+00	1.20E+00	1.15E+00	1.11E+00
CH3OH(g)	1.47E-05	3.00E-04	9.86E-04	1.11E-03	4.82E-04	1.00E-04	2.37E-05	7.14E-06	2.62E-06	1.12E-06	5.43E-07	2.91E-07	1.69E-07	1.05E-07	6.93E-08	4.78E-08
CHCl3(g)	4.94E-23	2.05E-19	8.53E-17	8.05E-15	2.55E-13	4.61E-12	5.06E-11	3.67E-10	1.93E-09	7.98E-09	2.71E-08	7.90E-08	2.03E-07	4.69E-07	9.96E-07	1.96E-06
Cl2(g)	9.58E-22	3.58E-17	5.21E-14	1.11E-11	6.44E-10	1.70E-08	2.39E-07	2.09E-06	1.27E-05	5.86E-05	2.17E-04	6.71E-04	1.80E-03	4.32E-03	9.36E-03	1.87E-02
CO(g)	1.01E-02	2.30E+00	1.04E+02	1.33E+03	4.54E+03	5.52E+03	5.60E+03	5.61E+03	5.61E+03	5.61E+03	5.61E+03	5.61E+03	5.61E+03	5.61E+03	5.61E+03	5.61E+03
CO2(g)	6.85E+02	1.03E+03	1.74E+03	1.73E+03	4.40E+02	3.54E+01	3.70E+00	5.86E-01	1.28E-01	3.58E-02	1.21E-02	4.81E-03	2.16E-03	1.07E-03	5.77E-04	3.34E-04
COCl2(g)	6.30E-20	2.85E-16	1.31E-13	1.06E-11	1.52E-10	6.82E-10	2.12E-09	5.39E-09	1.19E-08	2.33E-08	4.19E-08	6.99E-08	1.10E-07	1.64E-07	2.36E-07	3.26E-07

Table A-4. (continued).

T (C)	100	200	300	400	500	600	700	800	900	1,000	1,100	1,200	1,300	1,400	1,500	1,600
Species	Kmoles															
COF2(g)	1.12E-15	9.86E-14	3.37E-12	4.30E-11	1.55E-10	2.39E-10	3.16E-10	4.03E-10	5.01E-10	6.07E-10	7.22E-10	8.45E-10	9.76E-10	1.11E-09	1.26E-09	1.41E-09
H2(g)	2.30E+02	1.87E+03	4.89E+03	7.71E+03	1.00E+04	1.08E+04	1.10E+04	1.11E+04	1.11E+04	1.11E+04	1.11E+04	1.11E+04	1.10E+04	1.10E+04	1.10E+04	1.10E+04
H2O(g)	4.24E+03	3.55E+03	2.02E+03	8.28E+02	1.93E+02	2.65E+01	4.61E+00	1.09E+00	3.29E-01	1.20E-01	5.05E-02	2.40E-02	1.26E-02	7.11E-03	4.30E-03	2.75E-03
HCl(g)	1.30E+04	1.30E+04	1.30E+04	1.30E+04	1.30E+04	1.30E+04	1.30E+04	1.30E+04	1.30E+04	1.30E+04	1.30E+04	1.30E+04	1.30E+04	1.30E+04	1.30E+04	1.30E+04
HCOOH(g)	5.41E-07	1.48E-05	9.96E-05	1.96E-04	7.42E-05	7.45E-06	9.13E-07	1.64E-07	4.00E-08	1.23E-08	4.57E-09	1.96E-09	9.47E-10	5.03E-10	2.89E-10	1.78E-10
HF(g)	1.77E+02	1.77E+02	1.77E+02	1.77E+02	1.77E+02	1.77E+02	1.77E+02	1.77E+02	1.77E+02	1.77E+02	1.77E+02	1.77E+02	1.77E+02	1.77E+02	1.77E+02	1.77E+02
HNO3(g)	1.00E-36	1.00E-36	1.00E-36	1.00E-36	1.00E-36	1.00E-36	1.00E-36	1.00E-36	1.00E-36	1.00E-36	2.06E-36	1.23E-35	5.94E-35	2.41E-34	8.45E-34	2.62E-33
N2H4(g)	5.12E-28	2.30E-23	3.84E-20	9.14E-18	5.86E-16	1.68E-14	2.56E-13	2.40E-12	1.55E-11	7.56E-11	2.94E-10	9.52E-10	2.66E-09	6.60E-09	1.48E-08	3.05E-08
N2O4(g)	1.00E-36	1.00E-36	1.00E-36	1.00E-36	1.00E-36	1.00E-36	1.00E-36	1.00E-36	1.00E-36	1.00E-36	1.00E-36	1.00E-36	1.00E-36	1.00E-36	1.00E-36	1.00E-36
NH3(g)	1.13E+01	1.13E+01	1.13E+01	1.13E+01	1.13E+01	1.13E+01	1.13E+01	1.13E+01	1.13E+01	1.13E+01	1.13E+01	1.13E+01	1.13E+01	1.13E+01	1.13E+01	1.13E+01
NO(g)	1.00E-36	2.84E-31	4.46E-25	1.21E-20	1.41E-17	1.81E-15	7.96E-14	1.75E-12	2.31E-11	2.04E-10	1.33E-09	6.70E-09	2.77E-08	9.68E-08	2.94E-07	7.97E-07
NO2(g)	1.00E-36	1.00E-36	1.00E-36	1.00E-36	3.52E-33	1.65E-30	1.80E-28	8.31E-27	2.04E-25	3.07E-24	3.16E-23	2.39E-22	1.41E-21	6.78E-21	2.75E-20	9.65E-20
O2(g)	1.00E-36	1.00E-36	2.54E-36	8.09E-31	2.48E-27	2.72E-25	8.75E-24	1.47E-22	1.53E-21	1.12E-20	6.20E-20	2.74E-19	1.01E-18	3.20E-18	8.98E-18	2.27E-17

A-4. REFERENCES

Babad, Harry and Andrew G. Zeiler, 1973, "The Chemistry of Phosgene," *Chemical Reviews*, Vol. 73, No. 1, pp. 75–91.

Battin-Leclerc, F., F. Baronnet, G. Paternotte, J. P. Leclerc, and R. Gourhan, 2000, "Thermal Decomposition of Chloropicrin, Diphosgene and Phosgene Between 100 and 530 C," *Journal of Analytical and Applied Pyrolysis*, Vol. 53, No. 1, January, pp. 95–105.

Bond, B. D. and P. W. M. Jacobs, 1966, "The Thermal Decomposition of Sodium Nitrate," *Inorganic Physical Theory Journal Chemical Society A*, pp. 1265–1268.

Burrows, Ronald Bertram and Louis Hunter, 1932, "The Nitration of Halogenoethylenes," *Journal of the Chemical Society*, May, pp. 1357–1360.

Carey, G. F., R. T. McLay, and R. J. MacKinnon, 1993, "Finite-Element Modelling of In Situ Vitrification," *In Situ*, Vol. 17, No. 2, pp. 201–226.

Dick, John R., 2001, *Nitrate Explosives Tests to Support the Operable Unit 7-13/14 In Situ Vitrification Project,* INEEL/EXT-2001-00265, Rev. 0, Idaho National Engineering and Environmental Laboratory.

Dunlap, Kenneth L., 1996, "Phosgene," *Kirk-Othmer Encyclopedia of Chemical Technology*, Vol. 18, 4th Edition, Jacqueline I. Kroschwitz, exec. ed., and Mary Howe-Grant, ed., New York: John Wiley & Sons:, pp. 645–656.

EDF-3563, 2003, "Radiological Dose and Nonradiological Exposure Calculations for ISV Accident Scenarios," Rev. O, Idaho National Engineering and Environmental Laboratory.

EDF-3699, 2003, "Subsurface Processes During In-Situ Thermal Desorption of Buried Wastes at the SDA," Rev. 0, Idaho National Engineering and Environmental Laboratory.

Gaisinovich, M. S. and A. N. Ketov, 1969, "High-temperature Hydrolysis of Carbon Tetrachloride and Phosgene in the Gaseous Phase," *Russian Journal of Inorganic Chemistry*, Vol. 14, No. 9, pp. 1218–1220.

Gerberich, H. Robert and George C. Seaman, 1994, "Formaldehyde," *Kirk-Othmer Encyclopedia of Chemical Technology*, Vol. 11, 4th Edition, Jacqueline I. Kroschwitz, exec. ed., and Mary Howe-Grant, Ed., New York: John Wiley & Sons, pp. 929–951.

Hawley, Gessner G., 1981, *The Condensed Chemical Dictionary*, 10th Edition, San Francisco: Van Nostrand Reinhold Company.

Hickman, J. C., 1993, "Tetrachloroethylene," *Kirk-Othmer Encyclopedia of Chemical Technology*, Vol. 6, 4th Edition, Jacqueline I. Kroschwitz, exec. ed., and Mary Howe-Grant, ed., New York: John Wiley & Sons, pp. 50–59.

Hodgman, C. D., 1959, *Handbook of Chemistry and Physics,* 40th Edition, Chemical Rubber Publishing Co.

Holbrook, Michael T., 1993a, "Methylene Chloride," *Kirk-Othmer Encyclopedia of Chemical Technology*, Vol. 5, 4th Edition, Jacqueline I. Kroschwitz, exec. ed., and Mary Howe-Grant, ed., New York: John Wiley & Sons, pp. 1041–1050.

Holbrook, Michael T., 1993b, "Chloroform," *Kirk-Othmer Encyclopedia of Chemical Technology*, Vol. 5, 4th Edition, Jacqueline I. Kroschwitz, exec. ed., and Mary Howe-Grant, ed., New York: John Wiley & Sons, pp. 1051–1062.

Holbrook, Michael T., 1993c, "Carbon Tetrachloride," *Kirk-Othmer Encyclopedia of Chemical Technology*, Vol. 5, 4th Edition, Jacqueline I. Kroschwitz, exec. ed., and Mary Howe-Grant, ed., New York: John Wiley & Sons, pp. 1062–1072.

Jury, W. A., W. F. Spencer, and W. J. Farmer, 1983, "Behavior Assessment Model for Trace Organics in Soil: I. Model Description," *Journal of Environmental Quality*, Vol. 12, No. 4, October-December, pp. 558–564.

Jury, W. A., W. J. Farmer, and W. F. Spencer, 1984a, "Behavior Assessment Model for Trace Organics in Soil: II. Chemical Classification and Parameter Sensitivity," *Journal of Environmental Quality*, Vol. 13, No. 4, October–December, pp. 567–572.

Jury, W. A., W. F. Spencer, and W. J. Farmer, 1984b, "Behavior Assessment Model for Trace Organics in Soil: III. Applications of Screening Model," *Journal of Environmental Quality*, Vol. 13, No. 4, October–December, pp. 573–579.

Jury, W. A., W. F. Spencer, and W. J. Farmer, 1984c, "Behavior Assessment Model for Trace Organics in Soil: IV. Review of Experimental Evidence," *Journal of Environmental Quality*, Vol. 13, No. 4, October–December, pp. 580–586.

Kim, Hack Jin and Kwang Yui Choo, 1983, "Arrhenius Parameters for the Thermal Decomposition of Trichloroethylene," *Bulletin of Korean Chemical Society*, Vol. 4, No. 5, pp. 203–208.

Logsdon, John E., 2003, "Ethanol," In electronic version of *Kirk-Othmer Encyclopedia of Chemical Technology*, 4th Edition, John Wiley & Sons, URL http://www3.interscience.wiley.com/cgi-bin/mrwhome/104554789/HOME, downloaded on December 5, 2003.

Matzner, Markus, Raymond P. Kurkjy, and Robert J. Cotter, 1964, "The Chemistry of Chloroformates," *Chemical Reviews*, Vol. 64, pp. 645–687.

Mertens, James A., 1993, "Trichloroethylene," *Kirk-Othmer Encyclopedia of Chemical Technology*, Vol. 6, 4th Edition, Jacqueline I. Kroschwitz, exec. ed., and Mary Howe-Grant, ed., New York: John Wiley & Sons, pp. 40–50.

Mertens, Ralf, Clemens von Sonntag, Johan Lind, and Gabor Merenyi, 1994, "A Kinetic Study of the Hydrolysis of Phosgene in Aqueous Solution by Pulse Radiolysis," *Angewandte Chemie International Edition in English*, Vol. 33, No. 12, pp. 1259–1261.

Nerin, C., C. Domeno, R. Moliner, M. J. Lazaro, I. Suelves, and J. Valderrama, 2000, "Behavior of Different Industrial Waste Oils in a Pyrolysis Process: Metals Distribution and Valuable Products," *Journal of Analytical and Applied Pyrolysis*, Vol. 55, pp. 171–183.

ORNL, 1996, "Technical Evaluation of the In Situ Vitrification Melt Expulsion at the Oak Ridge National Laboratory, on April 21, 1996," Draft, Oak Ridge National Laboratory.

Outokumpu, 2003, *Outokumpu HSC Chemistry for Windows*, Oy, Finland: Outokumpu Research.

Ozokwelu, E. Dickson, 2003, "Toluene," *Kirk-Othmer Encyclopedia of Chemical Technology* (electronic version), 4th Edition, New York: John Wiley & Sons, URL: http://www3.interscience.wiley.com/cgi-bin/mrwhome/104554789/HOME, Downloaded on December 9, 2003.

Slaughterbeck, D. C., W. E. House, G. A. Freund, T. D. Enyeart, E. C. Benson Jr., and K. D. Bulmahn, 1995, *Accident Assessments for Idaho National Engineering Laboratory Facilities*, DOE/ID-10471, U.S. Department of Energy Idaho Operations Office.

Snedecor, Gayle, 1993, "Other Chloroethanes," *Kirk-Othmer Encyclopedia of Chemical Technology*, Vol. 6, 4th Edition, Jacqueline I. Kroschwitz, exec. ed., and Mary Howe-Grant, ed., New York: John Wiley & Sons, p. 17.

This page is intentionally left blank.

Appendix B

Detailed Discussion of the Potential Escape of Volatile Organics to Surrounding Ambient Soil

This page is intentionally left blank.

Appendix B

Detailed Discussion of the Potential Escape of Volatile Organics to Surrounding Ambient Soil

Volatile organics that vaporize in the transition zone (25–100°C) may migrate away from the melt front into the ambient zone rather than move toward the melt front and either pyrolyze or be transported to the off-gas hood by water vapor acting as carrier gas in the dry zone. Dragun (1991) asserts that volatiles are recondensed upon moving into the ambient zone, where concentration diffusion would then move them back toward the melt. Additionally, liquid–solid adsorption significantly impedes the movement of the recondensed chemicals through the ambient zone away from the melt. Consequently, Dragun (1991) concludes that volatile organics would be overtaken by the melt before making any appreciable movement through the ambient zone. Dragun (1991) used the soil transport model of Jury, Spencer, and Farmer (1983, 1984a, 1984b, 1984c) to estimate the migration speed of polychlorinated biphenyls (PCBs) in typical soil at room temperature to be 2.3E-05 cm/hour (75.5 years to migrate 6 in.). Such a slow migration speed caused Dragun (1991) to conclude that volatile chemicals like PCB would be overtaken by the melt progression before any appreciable migration through the ambient zone could occur.

Table B-1 shows results from applying the same model (Jury, Spencer, and Farmer 1983, 1984a, 1984b, 1984c) to several species in the waste buried in Operable Unit (OU) 7-13/14 within the Radioactive Waste Management Complex of the Idaho National Engineering and Environmental Laboratory. According to the model, the effective soil diffusion coefficient is expressed by Equations (B-5) and (B-6) of Jury, Spencer, and Farmer (1984a)

$$D_E = \frac{D_G^{air} K_H a^{10/3}/\phi^2 + D_L^{water}\theta^{10/3}/\phi^2}{\rho_b K_D + \theta + aK_H}$$, and the migration time is given by

$$t_D = l^2 / D_E \qquad \text{(B-1)}$$

where

l = Distance traveled

D_G^{air} = Gaseous diffusion coefficient in air

K_H = Henry's law constant in dimensionless form (concentration of solute in the vapor phase over that in the liquid phase)

a = Air content of the soil (equal to ϕ - θ)

ϕ = Porosity

D_L^{water} = Liquid diffusion coefficient in water

θ = Water content of the soil

ρ_b = Soil bulk density

K_D = Distribution coefficient and equal to $K_{oc} \times f_{oc}$, where K_{oc} is the distribution coefficient based on organic carbon content of the soil, and f_{oc} is the fraction of organic carbon in the soil.

Table B-1. Estimated migration in soil at 25°C. [a]

Species / INEEL Waste	Boiling Point	K_H	K_{oc}	Time (hour) Required to Diffuse 1 cm, f_{oc} = 0	f_{oc} = 0.005	f_{oc} = 0.0125	f_{oc} = 0.02	Migration Speed (cm/hour), f_{oc} = 0	f_{oc} = 0.005	f_{oc} = 0.0125	f_{oc} = 0.02
Benzene	80.1	0.22 [b]	0.083 [b]	0.0883	0.247	0.485	0.72	11.3	4.0	2.1	1.4
[illegible]	76.7	0.94 [b]	0.11 [b]	0.0379	0.087	0.16	0.24	26.4	11.5	6.2	4.3
Chloroform	61	0.12 [b]	0.029 [b]	0.143	0.245	0.397	0.55	7.0	4.1	2.5	1.8
Tetrachloroethylene	77	0.339 [c]	0.24 [d]	0.065	0.363	0.81	1.26	15.4	2.8	1.2	0.8
Toluene	110.6	0.270 [c]	—	0.076	—	—	—	13.2	—	—	—
Methylene chloride	40	0.123 [c]	—	0.14	—	—	—	7.1	—	—	—
1,1,1-Trichloroethane	68	0.736 [c]	—	0.042	—	—	—	23.8	—	—	—
Trichloroethylene	87.3	0.409 [c]	—	0.058	—	—	—	17.2	—	—	—
For Comparison	—	—	—								
PCB	—	0.0332 [e]	1.200 [e]	3,042				3.3E-04			
Chloroethene (vinyl chloride)	-13.37	97.0 [b]	0.40 [b]	0.023	0.024	0.027	0.0295	43.5	41.7	37.0	33.9

a. According to the model of Jury et al. (1983, 1984a, 1984b, 1984c), taking into account diffusion in the liquid and gas phase, vapor-liquid equilibrium, and liquid-solid adsorption. The distribution coefficient of the solute between the liquid and solid adsorbed phases, K_D, is equal to $K_{oc} \times f_{oc}$. When $f_{oc} = 0$, $K_D = 0$, and adsorption drops out of the equation. The K_{oc} is the distribution coefficient based on organic carbon content of the soil, and f_{oc} is the fraction of organic carbon in the soil. K_H is the Henry's law constant in dimensionless form (concentration of solute in the vapor phase over that in the liquid phase). The following parameters were taken from Jury et al. (1983): universal diffusion coefficient for organics in air = 0.43 m^2/day, and universal diffusion coefficient for organics in water = 4.3E-05 m^2/day. The following INEEL-specific model parameter values were assumed: porosity = 0.5, water volume fraction = 0.196, and soil bulk density = 1,140 kg/m^3.

b. From Jury et al. (1984b).

c. Calculated from dimensional Henry's law constants at 20°C given in Thomas (1982). $K_{H,dimensionless} = K_{H,atm \times m3/mol}/RT$, where R is the gas constant and equal to 8.206E-05 atm × m^3 × mol^{-1} × K^{-1}.

d. From Kenaga (1980).

e. From Dragun (1991). Gave value of 1.200 for K_D rather than separating the contributions of K_{oc} and f_{oc}, so the predicted diffusion time and migration speed shown here correspond to $K_{oc} = K_D$ and $f_{oc} = 1.0$ so that $K_{oc} \times f_{oc} = K_D$, allowing adsorption to be properly taken into account by the model.

INEEL = Idaho National Engineering and Environmental Laboratory
PCB = polychlorinated biphenyl

The organic carbon content in the soil at OU 7-13/14 is estimated to be 0.5–2.0% ($0.005 \leq f_{oc} \leq 0.02$). Migration was calculated at $f_{oc} = 0$ to estimate the limit when no adsorption occurs. Chloroethene (vinyl chloride) and PCB, although not in RMWC waste, were included for comparison because of their relatively high and low Henry's law constants, respectively. The higher the Henry's law constant, the greater is the solute's partitioning into the gas phase; and consequently, the more dominant the pore-air diffusion becomes as a pathway for transport and the adsorption becomes less of a factor.

Even organics like carbon tetrachloride and 1,1,1-trichloroethane that have pure boiling points at atmospheric pressure that are tens of degrees higher than room temperature (i.e., 76.7 and 68°C, respectively) have high partitioning into the vapor phase from the solute–water liquid mixture at 25°C. Consequently, it can be seen from Table B1 that the model of Jury, Spencer, and Farmer (1983, 1984a, 1984b, 1984c) predicts that such solutes will have high migration speeds due to high diffusion in the gas phase of the soil pores. The assertion of Dragun (1991) that volatile organics will condense upon reaching the ambient zone may be true for chemicals like PCB that have a low K_H value (0.033 for PCB), but it probably won't be for many of our volatiles, which means that adsorption may provide little resistance to transport through the ambient zone.

The rate of progression of the melt front has been estimated to be 2–10 cm/hour by Carey, McLay, and McKinnon (1993) and 3–6 cm/hour by Dragun (1991). The existence of buried inclusions, which is typical of OU 7-13/14, tends to inhibit convection and the melt growth (Carey, McLay, and McKinnon 1993). The movement of volatiles in the transition zone toward the dry zone could be impeded by a saturated water barrier within the 100°C isotherm (Farnsworth et al. 1999, Appendix C), and a gas-phase concentration gradient could exist to drive the volatiles into and through the ambient zone. The Jury model (Jury, Spencer, and Farmer 1983, 1984a, 1984b, 1984c) was created to rank the transport of species (i.e., determine relative transport speeds). However, the fact that the estimated transport times in absolute terms for several of our volatiles are on the same order of magnitude as the melt progression rate suggests that it is possible that the rate of migration of high-Henry's-law-constant species in the ambient zone through gas diffusion in pore air (if a driving concentration gradient is formed) could outpace the progression of the melt front.

REFERENCES

Carey, G. F., R. T. McLay, and R. J. MacKinnon, 1993, "Finite-Element Modelling of In Situ Vitrification," *In Situ*, Vol. 17, No. 2, pp. 201–226.

Dragun, James, 1991, "Geochemistry and Soil Chemistry Reactions Occurring During In Situ Vitrification," *Journal of Hazardous Materials*, Vol. 26, pp. 343–364.

Farnsworth, R. K., D. M. Henrikson, R. A. Hyde, D. K. Jorgensen, J. K. McDonald, D. F. Nickelson, M. C. Pfeifer, P. A. Sloan, and J. R. Weidner, 1999, *Operable Unit 7-13/14 In Situ Vitrification Treatability Study Work Plan*, DOE/ID-10667, Idaho National Engineering and Environmental Laboratory.

Jury, W. A., W. F. Spencer, and W. J. Farmer, 1983, "Behavior Assessment Model for Trace Organics in Soil: I. Model Description," *Journal of Environmental Quality*, Vol. 12, No. 4, October-December, pp. 558–564.

Jury, W. A., W. J. Farmer, and W. F. Spencer, 1984a, "Behavior Assessment Model for Trace Organics in Soil: II. Chemical Classification and Parameter Sensitivity," *Journal of Environmental Quality*, Vol. 13, No. 4, October–December, pp. 567–572.

Jury, W. A., W. F. Spencer, and W. J. Farmer, 1984b, "Behavior Assessment Model for Trace Organics in Soil: III. Applications of Screening Model," *Journal of Environmental Quality*, Vol. 13, No. 4, October–December, pp. 573–579.

Jury, W. A., W. F. Spencer, and W. J. Farmer, 1984c, "Behavior Assessment Model for Trace Organics in Soil: IV. Review of Experimental Evidence," *Journal of Environmental Quality*, Vol. 13, No. 4, October–December, pp. 580–586.

Kenaga, Eugene E., 1980, "Predicted Bioconcentration Factors and Soil Sorption Coefficients of Pesticides and Other Chemicals," *Ecotoxicology And Environmental Safety*, Vol. 4, No. 1, March, pp. 26–38.

Thomas, Richard G., 1982, "Volatilization From Water," Chapter 15, *Handbook of Chemical Property Estimation Methods - Environmental Behavior of Organic Compounds*, Warren J. Lyman, William F. Reehl, and David H. Rosenblatt, eds., New York: McGraw-Hill Book Company.

This page is intentionally left blank.

Appendix C

Alternative Initiators for Hypothetical Idaho National Engineering and Environmental Laboratory Melt Expulsion

This page is intentionally left blank.

Appendix C

Alternative Initiators for Hypothetical Idaho National Engineering and Environmental Laboratory Melt Expulsion

C-1. PURPOSE

A postulated melt expulsion is one of the accident scenarios to be examined in this engineering design file (EDF). The basis for this requirement is the experience of a melt expulsion at an ISV operation at Oak Ridge National Laboratory (ORNL) (ORNL 1996). The expulsion at ORNL was likely due to the rapid release of steam and energy from superheated water because the ISV operation took place in water-saturated soil above an impermeable rock layer. The potential for such a steam release may also exist at the waste storage pits and trenches being considered for in situ vitrification (ISV) at the Idaho National Engineering and Environmental Laboratory (INEEL). Nuclear probehole logging suggests that moisture in the waste zone is routinely 15–25 vol%. Observations of excavations at Pit 9 of the Subsurface Disposal Area within the Radioactive Waste Management Complex of the INEEL, using the glovebox excavator method, suggest that the underburden may be saturated in some areas. Some drums retrieved appeared to be waterlogged, and freestanding water was observed in the resulting void.[a]

Besides a gas bubble forming and growing under the melt, from either superheated water or other volatiles, the propulsive force needed to expel melt could come from the energetic conflagration of a mixture of pyrolysis gases and oxygen/nitrogen gas mixture formed from denitration of waste nitrate salts. The purpose of this appendix is to analyze these two possible initiators and their implications for off-gas release.

C-2. CASE 1—EXPULSION CAUSED BY AN EXPANDING BUBBLE

Soil and melt density data indicate that at the bottom of the melt (this analysis includes the underburden soil in the melt), the static pressure will be 15 psi above atmospheric. Thus, a bubble expanding and expelling melt will start at 15 psi (gauge) and expand to 0 psi (gauge), or from approximately 27 psi (absolute) to 12 psi (absolute). At melt temperature, the heat capacity (Cp) of an equivolume mixture of pyrolysis gases and denitration gases is approximately 12 Btu/lbmol °R. Cv is Cp-R, treating the mixture as an ideal gas, and is approximately 10 Btu/lbmol °R. Thus, the heat capacity ratio $\gamma = Cp / Cv$ is 1.2.

The work involved in adiabatically expanding a volume of gas V_1 from P_1 to P_2 is shown in Equation (C-1).

$$Work = -\frac{\gamma P_1 V_1}{\gamma - 1}\left[\left(\frac{P_2}{P_1}\right)^{\left(\frac{\gamma-1}{\gamma}\right)} - 1\right] . \qquad \text{(C-1)}$$

a. Thomas E. Bechtold Personal Communication to Todd T. Nichols, INEEL March 2, 2004 (EDF to be published).

Using the parameter values given above, for each cubic foot of gas starting at 27 psi (or 1.84 atm), the work derived by the expansion is 1.40 ft^3 atm (2,962.7 ft-lb_f).

The work required to lift the expelled melt is the weight times the distance lifted. Assuming a pit or trench depth of 12 ft, the melt must be elevated an average of half its depth to ground level, a distance of 6 ft. Consequently, the work required to lift a 20-ton mass of melt is 2.4×10^5 ft-lb_f (20 tons × 2,000 lb_m/ton × 1 lb_f/lb_m × 6 ft). From the energy per cubic foot (melt bottom conditions) released in the expansion, an initial bubble size of 81 ft^3 (2.4×10^5/2,963) is needed. This result is relatively insensitive to the heat capacity estimate and the resulting heat capacity ratio. Assuming the ideal gas law, an isothermal expansion would decrease the volume needed for the expansion to 75 ft^3. The equation for work from an isothermal expansion is given in Equation (C-2):

$$Work = -nRT \ln \frac{V_2}{V_1} \quad . \tag{C-2}$$

The actual volume required, therefore, would be within the range of 75–85 ft^3 (22–25 scf), with the number depending on the heat transfer from the melt to the bubble (or bubbles) undergoing the expansion. It is difficult to conceive a mechanism by which a bubble this size could form other than by the rapid expansion of superheated water—smaller bubbles would be expected to traverse the melt and release their energy of expansion more quietly (spattering small amounts of melt) before a bubble this size could form.

C-3. CASE 2—MELT EXPULSION THROUGH ENERGETIC COMBUSTION OF MIXED-PYROLYSIS AND DENITRATION GASES

A reaction of pyrolysis and oxygen-rich denitration gases could also provide the energy to expel the melt. The energy release per volume of pyrolysis gas will be based on the value for coke oven gas resulting from pyrolysis of wood (i.e., 500 Btu/ft^3 standard temperature and pressure). Cellulose, in contrast to oil, is a combination of carbohydrates rather than aliphatic compounds, so pyrolysis of cellulose will produce water as well as flammable compounds. Hence, the energy-per-unit volume of coke gas should be less than that for oil pyrolysis, and the calculated volume of gas needed to expel the melt will be larger than would be calculated for more energetic oil pyrolysis gases. As a result, the volume of gas released in an expulsion should be conservatively large using the coke-gas-energy value.

The products of pyrolysis of machine oil is given by Nerin et al. (2000) in terms of the moles of specific products generated per kilogram of oil. This is also referenced in S. Ashworth's original study of ISV off-gas.[b] A spreadsheet was constructed to calculate the oxygen required to combust these products and the water vapor and CO_2 formed by combustion. The spreadsheet shows that about 1 ft^3 of pure oxygen is needed per cubic foot of pyrolysis gas. Because this is almost exactly the ratio specified for coke pyrolysis gas (Hodgman 1959), which states that 5 ft^3 of air is needed to burn 1 ft^3 of coke gas. This similarity in oxygen requirements lends credence to the use of coke-gas combustion energy as an approximation to the combustion energy of the oil pyrolysis gas.

b. Ashworth, Samuel C., 2001, "Operable Unit 7-13/14 In Situ Vitrification Gas Generation (Draft)," INEEL/EXT-02-00269, Rev. A, INEEL.

One cubic foot of pyrolysis gas at melt temperature and melt-bottom pressure corresponds to 0.32 scf, so the combustion of 1 ft^3 of pyrolysis gas (at melt conditions) releases $0.32 \times 500 = 160$ Btu. Using the composition of the combustion-product gases and an estimate of the mixture-heat capacity (Reid [1977]), we estimate a temperature elevation to 3,358°C and a pressure of 9.3 atm for the after-combustion gaseous product at the same volume as the precombustion mix. The volume of mixed gases for combustion of the pyrolysis products is 2.33 ft^3 per cubic foot of pyrolysis gas. The additional 1.33 ft^3 includes 1.0 ft^3 O_2 and 0.33 ft^3 N_2, the ratio in gas formed during denitration of salts in the waste. Expanding 2.33 ft^3 of the product gas adiabatically to atmospheric pressure produces about one-quarter of the work required to elevate the melt. Hence, we estimate that 4 ft^3 of pyrolysis gas, mixed with 5.3 ft^3 of the O_2/N_2 mixture produced by denitration, is required to produce the energy to expel the melt.

This amount of pyrolysis gas is on the same order of magnitude as the gas volume contained in the voids in a waste drum at its approximate rupture pressure of 35 psi, so it is reasonable to assume a scenario in which a drum ruptures and introduces a sufficient volume of combustible gas to produce an energetic reaction that could expel significant melt. Although the corrosion rate of buried drums at RWMC is assumed to be high (EDF-ER-074; see footnote a), it is prudent to assume that some drums have remained unbreached and could rupture and provide sufficient combustible gas to produce an energetic reaction.

A pressurized drum rupture could leave some nonvolatile contaminants in the drum in a finely divided state. This finely divided material would have an increased probability of being swept out of the drum and carried through the melt in the resultant combustion reaction and volume of rising gas. The amount of finely divided contaminants, however, would be small because of the small quantity of fuel required for the combustion. For example, the amount of organic waste needed to be pyrolized to produce the combustible gas, both to pressurize the drum to rupture and to provide fuel for the subsequent energetic combustion, is minimal. One kilogram of machine oil pyrolyzes to form 0.058 moles of combustible gas, over ten times the amount of gas calculated to be needed for the combustion that could expel melt.

Nonvolatile contaminants could be added to a gas release due to a similar rupture of a drum containing nitrate-salt waste. Like the oil sludge waste, the mass of additional contaminants would be miniscule. In both cases, the amount of solids needed to release gas for the subsequent combustion would be very small (i.e., fractions of a kilogram).

REFERENCES

EDF-ER-074, 1999, "Potential Hydrogen-Related Concerns during Stage I, Phase II Drilling," Functional File No. INT-99-00596, Rev. 0, Idaho National Engineering and Environmental Laboratory.

Nerin, C., C. Domeno, R. Moliner, M. J. Lazaro, I. Suelves, and J. Valderrama, 2000, "Behavior of Different Industrial Waste Oils in a Pyrolysis Process: Metals Distribution and Valuable Products," *Journal of Analytical and Applied Pyrolysis*, Vol. 55, pp. 171–183.

ORNL, 1996, "Technical Evaluation of the In Situ Vitrification Melt Expulsion at the Oak Ridge National Laboratory, on April 21, 1996," Draft, Oak Ridge National Laboratory.

Reid, R., 1977, *Properties of Gases and Liquids*, Third Edition, New York: McGraw-Hill Book Co.